The stable states picture of chemical reactions. II. Rate constants for condensed and gas phase reaction models

Richard F. Grote and James T. Hynes

Citation: J. Chem. Phys. **73**, 2715 (1980); doi: 10.1063/1.440485
View online: http://dx.doi.org/10.1063/1.440485
View Table of Contents: http://jcp.aip.org/resource/1/JCPSA6/v73/i6
Published by the AIP Publishing LLC.

The stable states picture of chemical reactions. II. Rate constants for condensed and gas phase reaction models[a)]

Richard F. Grote and James T. Hynes[b)]

Department of Chemistry, University of Colorado, Boulder, Colorado 80309
(Received 2 May 1980; accepted 6 June 1980)

The time correlation function (tcf) formulas for rate constants κ derived via the stable states picture (SSP) of chemical reactions are applied to a wide variety (a–d) of gas and solution phase reaction models. (a) For gas phase bimolecular reactions, we show that the flux tcf governing κ corresponds to standard numerical trajectory calculation methods. Alternate formulas for κ are derived which focus on saddle point surfaces, thus increasing computational efficiency. Advantages of the SSP formulas for κ are discussed. (b) For gas phase unimolecular reactions, simple results for κ are found in both the strong and weak coupling collision limits; the often ignored role of product stabilization is exposed for reversible isomerizations. The SSP results correct some standard weak coupling rate constant results by as much as 50%. (c) For barrier crossing reactions in solution, we evaluate κ for a generalized (nonMarkovian) Langevin description of the dynamics. For several realistic models of time dependent friction, κ differs dramatically from the popular Kramers constant friction predictions; this has important implications for the validity of transition state theory. (d) For solution reactions heavily influenced by spatial diffusion, we show that the SSP isolates short range reaction dynamics of interest and includes important barrier region effects in structural isomerizations often missed in standard descriptions.

I. INTRODUCTION

In the preceding paper[1] (hereafter I), Northrup and Hynes showed how chemical reaction rate constants are related to molecular dynamics by time correlation function (tcf) formulas. This was accomplished via the stable states picture (SSP), in which attention is focused on the dynamical flux out of a stable reactant region and the ensuing flux into a stable product region. The rate constant is determined by the dynamics in an intermediate, or "barrier," region located between these two stable states.

In this paper, we demonstrate the power and range of this approach by determining rate constants for a wide variety of reaction models. These range from gas phase bimolecular and unimolecular reactions to condensed phase potential barrier crossing and diffusion-controlled reactions. This work continues and significantly extends prior work in this direction by Northrup and Hynes.[2–5] Our present efforts provide insight on major features of importance for various reaction models and lead to some significant new results. The major example presented here is a new rate constant result for condensed phase barrier crossing based on a fairly realistic description of dynamical interactions with the solvent.

To keep this paper relatively self-contained, we briefly list and discuss some of the tcf rate constant formulas derived in I. The stable states picture (SSP) focuses on three regions. The first two describe the stable reactants (R) and stable products (P). These regions are separated by a high energy intermediate or barrier region (I). There are thus two dividing surfaces S_R and S_P associated with R and P, respectively. The forward (f) reaction rate constant is the barrier rate constant

$$\kappa_f = \int_0^\infty dt \langle j_i(S_R) j_o^*(S_P, t) \rangle_R \ . \tag{1.1}$$

This tcf expression involves (a) the inward flux $j_i(S_R)$ from R into I across S_R and (b) the outward flux $j_o(S_P)$ from I into P across S_P. The asterisk superscript denotes the dynamical condition that no recrossing into region I is allowed for trajectories that have crossed S_R or S_P from I into the stable reactant or product regions. Thus, κ_f is determined by short-lived nonequilibrium dynamics occurring in region I and *not* by the slowly varying R and P populations.

The brackets $\langle(\cdots)\rangle_R$ in Eq. (1.1) denote an equilibrium average over initial conditions of (a) any buffer gas or solvent molecules present and (b) the atoms and molecules participating in the reaction. The subscript R denotes a normalization of the latter by the reactants' partition function Q_R. The equilibrium average arises from the key SSP assumption of internal equilibrium in the stable reactants.

There are several equivalent ways of writing κ_f.[1] Two important alternate forms are

$$\kappa_f = \langle j_i(S_R) \rangle_R + \int_0^\infty dt \langle j_i(S_R) j_o^*(S_R, t) \rangle_R \ , \tag{1.2}$$

which focuses solely on fluxes across the reactant surface (cf. Sec. III of I) and

$$\kappa_f = \int_0^\infty dt \langle j_i(S_R) j^*(S, t) \rangle_R \ , \tag{1.3}$$

which involves the *total* flux j at some arbitrary dividing surface S lying within I and away from S_R and S_P (cf. Sec. III of I).

Expressions analogous to Eqs. (1.1)–(1.3) hold for reverse rate constants κ_r. Since κ_f and κ_r are simply related by $\kappa_f = K^{eq}\kappa_r$, where K^{eq} is an equilibrium constant, we consider only forward reactions.

The identification of κ_f as the true reaction rate con-

[a)]Supported in part by the National Science Foundation and the Alfred P. Sloan Foundation.
[b)]John Simon Guggenheim Memorial Fellow, 1979. University of Colorado CRCW Faculty Fellow, 1979.

 0021-9606/80/182715-18$01.00

stant depends on the SSP assumption of rapid internal equilibration in the reactant and product regions.[1] This allows (a) the restriction of the flux into region I to be that flux arising from an equilibrium reactant distribution and (b) the neglect of events occurring *after* passage into the stable product is accomplished.

The rapid equilibration assumption breaks down in a few important cases. Slow internal equilibration within the stable reactant and product states can then influence the rate. According to the SSP,[1,3-5] the rate constant in this case is modified to

$$k_f = [1 + (\kappa_f/\kappa_R)]^{-1}\kappa_f \tag{1.4}$$

for an irreversible reaction and to

$$k_f = [1 + (\kappa_f/\kappa_R) + (\kappa_r/\kappa_P)]^{-1}\kappa_f \tag{1.5}$$

for a reversible reaction.[6] Here κ_R and κ_P are *internal relaxation* rate constants governing equilibration rates within R and P, respectively. They are related to tcf's of population fluctuations at the stable state surfaces in Sec. IV of I. When $\kappa_R \lesssim \kappa_f$, the rate depends significantly on dynamics within the stable reactant. The rate of "flow" up to surface S_R can compete with the passage rate from S_R to S_P governed by κ_f. When $\kappa_P \lesssim \kappa_r$, the rate can depend significantly on the equilibration rate in the stable product. This equilibration can compete with the passage *back* to reactants ($S_P \to S_R$) governed by κ_r. When $\kappa_f \ll \kappa_R$ and $\kappa_r \ll \kappa_P$, these two phenomena are negligible and we recover the barrier rate constant κ_f.

The outline of this paper is as follows: Sections II and III deal with gas phase reaction models. Bimolecular reactions are discussed in Sec. II, while Sec. III deals with unimolecular reactions in two extreme limits of energy transfer. In Sec. IV, we turn to reactions in solution and evaluate rate constants for fairly realistic models of dynamical interaction with the solvent. In Sec. V, we consider reactions for which slow spatial diffusion plays a key role. We attempt to illustrate the key features and important directions for future extensions in each section. Section VI provides a summary.

II. GAS PHASE BIMOLECULAR REACTIONS

In this section, we apply our tcf formulas for rate constants to bimolecular gas phase reactions. We relate our SSP results to more standard expressions and indicate some advantages of our own formulation.

A. Collision viewpoint

Our tcf expression [Eq. (1.1)] for κ_f, i.e.,

$$\kappa_f = \int_0^\infty dt\, \langle j_i(S_R) j_o^*(S_P, t)\rangle_R \,, \tag{2.1}$$

has a simple and direct correspondence with (classical) collisional trajectory calculations for gas phase bimolecular reactions. To see this, we consider a standard representation in Fig. 1 for a collinear atom-transfer reaction[7]:

$$A + BC \to AB + C \,.$$

The reactant and product surfaces are placed away from the interaction zone I. They are thus located in the

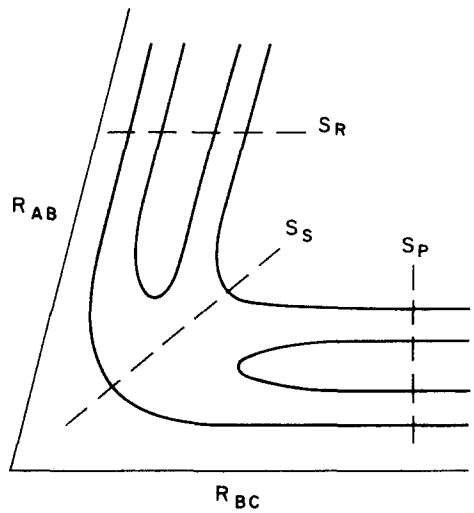

FIG. 1. Potential surface diagram for a collinear A + BC reaction. The dividing surfaces discussed in the text are displayed.

asymptotic reactant (R) and product (P) regions. Trajectories crossing S_R into I are sampled from an equilibrium distribution of reactants. Such trajectories are then followed throughout a collision until either (a) products are formed by crossing of S_P (AB and C separate) or (b) reactants are reformed by crossing of S_R (A and BC separate). This corresponds *precisely* to our SSP discussion of Eq. (2.1) in Sec. II of I and Sec. I.

Since no forces here *return* reactants or products to the intermediate zone, the absorbing boundary conditions in the dynamics in Eq. (2.1) are moot. Then Eq. (2.1) takes the simpler form

$$\kappa_f = \int_0^\infty dt\, \langle j_i(S_R) j_o(S_P, t)\rangle_R \,, \tag{2.3}$$

where now there are no restrictions on the dynamics.[8] This is the simplest tcf formula for the rate constant from the collision point of view. With suitable quasiclassical definitions of the internal quantum states of reactants and products, the state-to-state rate constant analogs of Eq. (2.3) can also be derived.[9]

A more familiar expression for the rate constant obtained from the "collision" viewpoint is the equilibrium average[10]

$$\kappa_f = \langle j_i(S_R)\chi(S_R)\rangle_R \,. \tag{2.4}$$

Here the characteristic function $\chi(S_R)$ equals unity if a trajectory originating from reactants is reactive; it equals zero if the trajectory is nonreactive. We can demonstrate the identity of Eqs. (2.3) and (2.4) as follows: We first rewrite Eq. (2.3) as

$$\kappa_f = \int_0^\infty dt\, \langle j_i(S_R) j(S_P, t)\rangle_R \,. \tag{2.5}$$

This replacement of the outward flux $j_o(S_P, t)$ by the *total* flux $j(S_P, t)$ across the product surface is exact because (a) all trajectories arise from reactants and (b) no forces return separated products to the intermediate region. The time integral of the flux $\int_0^\infty dt\, j(S_P, t)$ in Eq. (2.5) is just $\chi(S_R)$; contributing trajectories must arise from the reactants and ultimately form products. This estab-

lishes the equivalence of Eqs. (2.3) and (2.4).

There are at least two advantages of the tcf (2.3) (and its state-to-state analogs) over Eq. (2.4). First, the flux tcf itself as a function of time gives a more detailed picture of reactive dynamics than does its integrated time area κ_f. Since the tcf involves *some* averaging over initial conditions, its information content lies between that of the enormous detail of individual trajectories and that of the fully averaged and time independent rate constant. Second, we will develop evaluation techniques in Sec. IV for the rate constant where the reactant motion is coupled to that of a liquid solvent. Similar techniques can account for the effect on motion in the reaction coordinate of intramolecular degrees of freedom orthogonal to this coordinate.[11] This is under study.[12]

B. Saddle point initial conditions

The collision viewpoint is sometimes inconvenient. Many trajectories originating from reactants may recross S_R, i.e., are unreactive. From a computational viewpoint then, the collision picture can often be inefficient; only a small fraction of these trajectories are "interesting," i.e., reactive.

An alternate perspective which circumvents this difficulty to some extent was developed by Keck[13] and Anderson[14] and has been discussed by a number of authors.[15] The basic idea is to relate the rate constant to the fate of trajectories *originating* from the saddle point. While the population in this region is low, many such trajectories lead to reaction, thereby increasing computational efficiency.[13–15] Our tcf expressions for rate constants will now be cast in this "saddle point" or "transition state" language.

We begin with Eq. (1.3) for κ_f rewritten as

$$\kappa_f = \int_0^\infty dt \langle j_i(S_R) j(S_S, t)\rangle_R \ . \tag{2.6}$$

Here S_S denotes a saddle point dividing surface (Fig. 1). We have again used the fact that the absorbing BC's are moot to write $j^*(S_S, t) = j(S_S, t)$ in Eq. (2.6) (i.e., unrestricted dynamics). We next bring the propagator in $e^{iLt} j(S_S)$ in Eq. (2.6) around to the left in the average and reverse the momenta to find that

$$\kappa_f = \int_0^\infty dt \langle j(S_S) j_i(S_R, -t)\rangle_R = \int_0^\infty dt \langle j(S_S) j_o(S_R, t)\rangle_R \ . \tag{2.7}$$

Equation (2.7) does not yet involve the saddle point flux and the flux into the product zone. Its form, however, suggests that the *reverse* rate constant κ_r can be related to the form we wish. Indeed, similar manipulations of the formula

$$\kappa_r = \int_0^\infty dt \langle j_i(S_P) j(S_S, t)\rangle_P \tag{2.8}$$

give the expression

$$\kappa_r = \int_0^\infty dt \langle j(S_S) j_o(S_P, t)\rangle_P \ . \tag{2.9}$$

Now, since the ratio κ_f/κ_r is the equilibrium constant K^{eq}, i.e.,

$$\kappa_f = K^{eq} \kappa_r \tag{2.10}$$

and the reactant and product averages are related by $\langle(\cdots)\rangle_R = K^{eq}\langle(\cdots)\rangle_P$, we can combine Eq. (2.9) with Eq. (2.10). This gives the desired result for the forward rate constant

$$\kappa_f = \int_0^\infty dt \langle j(S_S) j_o(S_P, t)\rangle_R \tag{2.11}$$

or its equivalent

$$\kappa_f = \int_0^\infty dt \langle j(S_S) j(S_P, t)\rangle_R \ . \tag{2.12}$$

Similarly, combination of Eqs. (2.7) and (2.10) gives the reverse rate constant as

$$\kappa_r = \int_0^\infty dt \langle j(S_S) j(S_R, t)\rangle_P \ . \tag{2.13}$$

Equations (2.12) and (2.13) give the desired rate constant expressions in terms of the tcf's of (a) an initial flux across the saddle point and (b) the subsequent flux across one of the stable state surfaces. They provide very efficient computational routes to the calculation of rate constants.[16]

The saddle point analog of the collision picture expression (2.4) has also been discussed.[10] It is given by

$$\kappa_f = \langle j(S_S)\chi(S_S)\rangle_R \ . \tag{2.14}$$

The characteristic function $\chi(S_S)$ equals unity if a trajectory starting on the surface S_S ultimately exits to region P. Otherwise, $\chi(S_S)$ equals zero. Equations (2.14) follows directly from our Eq. (2.12) by the identity $\int_0^\infty dt\, j(S_P, t) = \chi(S_S)$ in this equation.

C. Connection to transition state theory

Yet another tcf representation of κ_f is useful in the discussion of transition state theory (TST).[17] Since the rate constant is independent of any choice of dividing surface in the intermediate zone (cf. Sec. III of I), we can just as well write Eq. (2.12) as[18]

$$\kappa_f = \int_0^\infty dt \langle j(S_S) j(S_S, t)\rangle_R \ . \tag{2.15}$$

TST focuses on the saddle point surface; it is assumed that no trajectory crossing S_S from the side containing R towards the side containing P recrosses S_S.[3,10,16,17] Then $\kappa_f \equiv \kappa_f^{TST}$ is determined *solely* by the initial delta function singularity in the flux tcf $\langle j(S_S) j(S_S, t)\rangle_R$ arising from those trajectories crossing S_S initially from the side of R to the side of P.[19] This relationship of κ_f^{TST} to a tcf singularity was evidently first pointed out by Zwanzig[20] and has been discussed in a number of contexts.[3,21]

It is often stated that TST is exact if there is no recrossing of a surface located in what we have called the intermediate zone. This statement must be carefully interpreted; its validity requires an equilibrium distribution of those particles that actually cross the surface.[22] This condition is often violated[22] in, e.g., gas phase unimolecular reactions, to which we now turn.

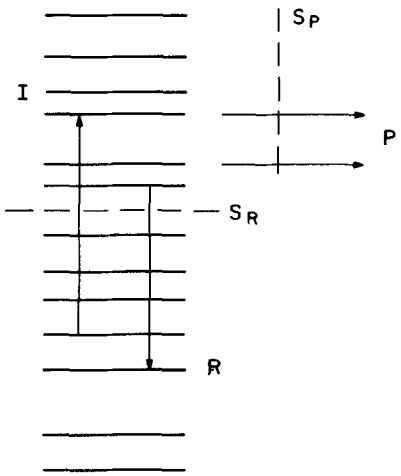

FIG. 2. Schematic model for unimolecular decomposition. Only a very few of the possible levels and transitions are shown. The first level in I has the threshold energy value E_0.

III. GAS PHASE UNIMOLECULAR REACTION MODELS

Many unimolecular reactions can be characterized as escape from a potential energy well.[23,24] Once the molecular energy exceeds some threshold, reaction can occur irreversibly unless deactivating collisions with surrounding buffer gas molecules intervene and return the molecule to the well. The reaction is then conveniently discussed in terms of (a) intrinsic reaction steps of those molecules with sufficient energy to react and (b) collisional activating and deactivating steps for their formation and depletion. We now show how our SSP formulation describes such reactions.

A. Strong coupling limit

We focus first on the *strong coupling* limit where large amounts of energy can be exchanged upon collision.

1. Irreversible decomposition

A well-known schematic model for unimolecular decomposition is displayed in Fig. 2. Collisions of the molecule with surrounding buffer gas molecules M transfer the molecule from and to energy levels of its stable chemical state R to and from its high energy reactive states in R^*, here labeled I:

$$R(i) + \mathrm{M} \underset{\omega_{ji}}{\overset{\omega_{ij}}{\rightleftharpoons}} R^*(j) + \mathrm{M} \ . \tag{3.1}$$

The intermediate region I states begin above a threshold energy E_0. A molecule in some state i within I may unimolecularly decompose to produce product P with a unimolecular rate constant ω_{iP}:

$$R^*(i) \xrightarrow{\omega_{iP}} P \ . \tag{3.2}$$

Here the rate constants ω_{iP} are regarded as known or to be modeled.[25] As in Sec. II, we could consider tcf expressions for these quantities. Here, however, we are one level removed from such a microscopic description. We characterize the reaction via master, or kinetic, equations[13,26]:

$$\partial \rho_i / \partial t = -\sum_j \omega_{ij}\rho_i + \sum_j \omega_{ji}\rho_j - \omega_{iP}\rho_i \ . \tag{3.3}$$

Our task is then to evaluate the rate constant at this level by regarding R and P as the stable states and the excited states R^* as comprising the intermediate region I.

We consider this model first in the so-called *strong collision* limit.[27] Then the collisional transition probabilities (rates) from any state i to another state j are[24]

$$\omega_{ij} = Z\rho_j^{eq} \ . \tag{3.4}$$

Here Z is the collision frequency; ρ_j^{eq} is the j state equilibrium probability $\rho_j^{eq} = e^{-\beta E_j}/Q$, where $Q = Q_R + Q_I$ is the partition function for the molecule. The total collisional loss L_i from level i, of population ρ_i, then depends only upon the collision frequency and the level population:

$$L_i = -\sum_j \omega_{ij}\rho_i = -Z\rho_i \ . \tag{3.5}$$

A simple steady state solution[28] of Eqs. (3.3) and (3.4) shows that the reactant R levels remain in internal equilibrium; the levels in I, however, generally have some *nonequilibrium* distribution due to the perturbation of reactive loss. Along with the irreversible passage into the P region, this precisely matches the SSP viewpoint.

We evaluate the rate constant equation (1.1):

$$\kappa_f = \int_0^\infty dt \langle j_i(S_R) j_o^*(S_P, t)\rangle_R \tag{3.6}$$

for this model in Appendix A. For the usual case of reaction threshold energy large compared to thermal energy ($\beta E_0 \gg 1$), we find that

$$\kappa_f = \sum_{i\in I} \rho_i^{eq} Z \omega_{iP} (Z + \omega_{iP})^{-1} \ . \tag{3.7}$$

This is, of course, the well-known RRKM form.[23,24,29] At high collision frequency, equilibrium prevails in I and $\kappa_f \to \sum_{i\in I}\rho_i^{eq}\omega_{iP}$. This TST-like result involves the production rates for the product as weighted by an equilibrium distribution in I. At intermediate and low densities, partial to major nonequilibrium obtains in I. This is reflected in Eq. (3.7) by the effective I region distribution $Z\rho_i^{eq}(Z + \omega_{iP})^{-1}$. In the extreme low density limit, region I is drastically depleted of population. This allows a major simplification in the rate constant description to which we now turn.

2. Low density collision-dominated limit

In the very low density limit, the rate constant is determined solely by the rate limiting activation steps to region I. For example, the strong collision model result Eq. (3.7) gives

$$\kappa_f \to \sum_{i\in I} Z\rho_i^{eq} = \sum_j \sum_{i\in I} \omega_{ij}\rho_i^{eq} \ . \tag{3.8}$$

This can be rewritten as

$$\kappa_f = \sum_j \sum_{i\in I} \rho_j^{eq}\omega_{ji} \approx \sum_{j\in R} \sum_{i\in I} \rho_j^{eq}\omega_{ji} \tag{3.9}$$

with detailed balance, when $\beta E_0 \gg 1$. Therefore, the low density rate constant is the equilibrium (*in R*) rate of production of the energetic intermediate states.

We can establish this as a general feature from the alternate rate constant formulation (1.2):

$$\kappa_f = \langle j_i(S_R)\rangle_R + \int_0^\infty dt \langle j_i(S_R) j_o^*(S_R, t)\rangle_R \ . \tag{3.10}$$

In the low density limit, all molecules promoted to the intermediate region decompose *before* they suffer a deactivating collision. We can therefore neglect the second member of Eq. (3.10); there will be vanishing *return* flux $j_o^*(S_R, t)$ to the stable reactant. The rate constant is then given by the initial, short time contribution

$$\kappa_f \approx \langle j_i(S_R)\rangle_R \ , \tag{3.11}$$

i.e., the production rate of energized molecules from an equilibrium distribution in the stable reactant. In terms of quantum levels and general transition probabilities W_{ij}, this is

$$\kappa_f = \sum_{i\in R}\sum_{j\in I} \rho_i^{eq} W_{ij} \ , \tag{3.12}$$

which generalizes Eq. (3.9). In terms of a classical description of energy transfer in terms of a transition rate kernel $K(\epsilon \to \epsilon')$, this is

$$\kappa_f = \int_0^{E_0} d\epsilon \ \rho_R^{eq}(\epsilon) \int_{E_0}^\infty d\epsilon' \, K(\epsilon \to \epsilon') \ , \tag{3.13}$$

first obtained by Bak and co-workers[30] (see also Ref. 31).

In the strong coupling limit, internal equilibrium is maintained in the stable reactant state *below* the threshold energy. We now turn to the *weak coupling* limit where this equilibrium assumption breaks down to some extent; a slightly different stable state definition is required.

B. Dissociation via energy diffusion

Our final low density model, due to Kramers,[32] is for dissociative escape from a potential well (Fig. 3). The reaction is viewed as a slow and rate determining *diffusion* in energy of an oscillator up to a dissociation energy E_d; the oscillator then rapidly dissociates. The SSP approach can be applied to this model by (a) recognizing the irreversible flux across the energy surface $E = E_d$ and (b) finding an energy surface in the reactant well below which internal equilibrium holds.

Slow energy diffusion via weak collisions is clearly the opposite extreme of the strong coupling limit of Sec. III A. It is most appropriate for massive diatomics immersed in gases of small, light molecules.[33] It also has relevance for gas phase ion recombination,[34(a)] molecular sticking on surfaces,[34(b)] and possibly intramolecular energy flow.[35]

1. Model for dissociation

The specific model assumptions are (a) the time between oscillator (O)–gas molecule (M) collisions is large compared to characteristic oscillator periods ω^{-1};

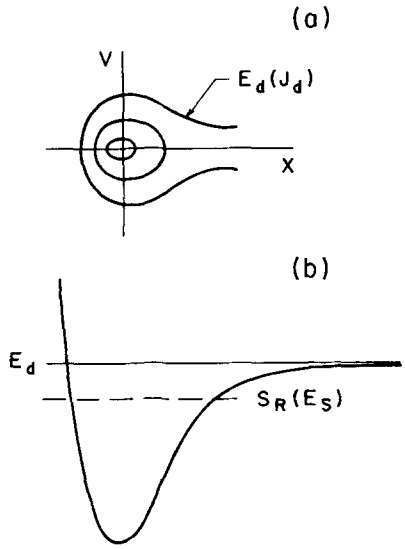

FIG. 3. Schematic definition diagrams for dissociation of a Morse oscillator. (a) Phase curves, including that for dissociation. (b) Potential energy curve indicating the stable reactant surface S_R.

the phase of O is then "randomized" between O–M collisions; (b) the energy of O is only *very slightly* changed per collision; (c) on the phase curve of O at energy E_d, *rapid* irreversible passage to products occurs by an unstable oscillation; the true unimolecular dissociation rate then plays no role in the reaction rate constant.

The reaction rate constant will then be proportional to a "friction constant" ζ governing energy transfer to and from O. The constant ζ is proportional to the mean square energy transfer per collision and the gas density.[24(a)] This is the low density bimolecular limit of a unimolecular reaction.

With the above assumptions, Kramers[32] derived an approximate diffusion equation in action (J) space for the oscillator probability distribution $\rho(J, t)$:

$$\partial\rho(J,t)/\partial t = -(\partial/\partial J) j(J,t) = \frac{\partial}{\partial J}\left\{D(J)\left[\frac{\partial}{\partial J} + \beta\omega(J)\right]\right\}\rho(J,t) \ . \tag{3.14}$$

The flux in action is $j(J, t)$; the action itself is the integral

$$J(E) = (2\pi)^{-1} \oint dx \, p \tag{3.15}$$

of the momentum over an orbit at fixed energy. The oscillator frequency is $\omega(J) = \partial E/\partial J$; the action diffusion coefficient is

$$D(J) = [\beta\omega(J)]^{-1}\zeta J \ . \tag{3.16}$$

The rapid reactive step proper is accounted for by the absorbing boundary condition (BC)

$$\rho(J_d, t) = 0 \ , \tag{3.17}$$

where $J_d = J(E_d)$ is the action at dissociation.

We will consider two oscillator models. The first is a truncated harmonic oscillator (HO), for which

$$\omega = \omega_0 = \text{constant}, \quad E(J) = \omega_0 J \le E_d \ . \tag{3.18}$$

The second and more realistic model is the anharmonic Morse oscillator (MO), for which[36,37]

$$\omega(J) = \omega_0[1 - (\omega_0 J/2E_d)] ,$$
$$E(J) = E_d[1 - (\omega/\omega_0)^2 . \quad (3.19)$$

Kramers obtained approximate rate constants for the well escape problem for a high threshold $\beta E_d \gg 1$[32,38-40]:

$$\kappa_f^{\mathrm{Kr}} = \zeta \beta E_d e^{-\beta E_d} \ (\mathrm{HO}) , \quad (3.20a)$$
$$\kappa_f^{\mathrm{Kr}} = 2\zeta \beta E_d e^{-\beta E_d} \ (\mathrm{MO}) . \quad (3.20b)$$

These provide a useful comparison for our own results.

2. Dissociation rate constants

Reaction from the threshold energy E_d severely depletes the population of high energy oscillators. This nonequilibrium suppression (Fig. 4) can extend to energies significantly below E_d. Well *away* from E_d, however, the energy distribution is essentially its equilibrium form. For *large* threshold energy ($\beta E_d \gg 1$), this leaves a significant energy range where internal equilibrium holds. Together with the irreversible flux condition across the surface $E = E_d$, this exactly matches the SSP viewpoint.

We therefore consider the barrier rate constant for dissociation

$$\kappa_f = \int_0^\infty dt \langle j_i(J_s) j_o^*(J_d, t) \rangle_R \quad (3.21)$$

[cf. Eq. (1.1)]. The intermediate region I is defined by the threshold action $J_d(E_d)$ and the action $J_s(E_s)$ at the reactant stable state surface (cf. Fig. 3).

The action flux tcf integral equation (3.21) can be evaluated by methods developed by Northrup and Hynes[4]; the details are sketched in Appendix B. Our result for the rate constant is

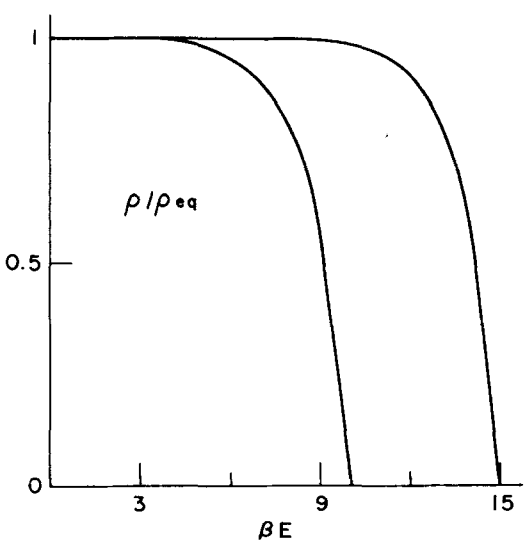

FIG. 4. Ratio ρ/ρ^{eq} of the Morse oscillator internal energy distribution to its equilibrium value versus reduced energy βE. Leftmost curve: $\beta E_d = 10.0$; rightmost curve; $\beta E_d = 15$. These curves were found by an approximate steady state solution of Eqs. (3.14)–(3.17).

TABLE I. Dissociation rate constants, divided by $\zeta e^{-\beta E_d}$, for the harmonic oscillator (HO) and Morse oscillator (MO) for various dimensionless dissociation energies βE_d.

	βE_d	κ_f [a]	κ_f^{num} [b]	κ_f^{Kr} [c]	k_f [d]
HO	10	9.1	8.9	10.0	8.9
	15	13.9	13.9	15.0	13.9
	20	18.9	18.9	20.0	18.9
MO	10	13.2	12.9	20.0	12.8
	15	21.7	...	30.0	21.7
	20	30.6	31.3	40.0	30.6

[a]Calculated from Eq. (3.22).
[b]From Ref. 39.
[c]Calculated from Eq. (3.20).
[d]Calculated from Eq. (3.30).

$$\kappa_f = \left[Q(E_s) \int_{J_s}^{J_d} dJ R(J) \right]^{-1} . \quad (3.22)$$

Here $R(J)$ is a local "resistance" to action flow

$$R(J) = [D(J) e^{-\beta E(J)}]^{-1} , \quad (3.23)$$

and the reactant partition function is

$$Q(E_s) = \int_0^{J_s} dJ e^{-\beta E(J)} = \int_0^{E_s} dE \omega^{-1}(E) e^{-\beta E} . \quad (3.24)$$

For each oscillator model and for a given E_d, the stable state reactant surface J_s, and thus E_s, was varied to minimize κ_f.[4] We find that $\kappa_f(E_s)$ has a very wide E_s range for which κ_f assumes very nearly its minimum value, which we adopt. The results are shown in Table I.

Our results are in excellent agreement with those of Bak and Andersen,[39] who numerically integrated the diffusion equations (3.14) and (3.17). Kramers' Eq. (3.20a) is quite good for the (unrealistic) harmonic case (5%–10% error). In contrast, Kramers' result [Eq. (3.20b)] is in error by 30%–50% for the nonlinear Morse oscillator. A major source of this error can be seen from Eqs. (3.22) and (3.23). The integral over region I is proportional to $\int_{E_s}^{E_d} dE J^{-1}(E) e^{\beta E}$. If $J(E)$ is approximated by its threshold value $J_d = 2E_d/\omega_0$, then Eq. (3.20b) follows. Evidently, the E dependence of J over all of region I is important and is correctly handled in the SSP result κ_f.

3. Nonequilibrium in the stable state

We now consider the *low* threshold case ($\beta E_d \lesssim 5$). Nonequilibrium suppression of the energy distribution by reactive loss at E_d now spreads very far down into the oscillator stable state R. Thus, internal equilibrium *no longer* holds in R. According to the SSP, the rate constant for dissociation will now depend both on (a) the barrier rate constant κ_f [Eq. (3.22)] *and* (b) the internal equilibration rate within R. The latter is governed by (cf. Sec. I and Sec. IV of I)

$$\kappa_R = \left\{ \rho_{eq}^{-1}(J_s) \int_0^\infty dt [\rho^0(J_s, t | J_s) - \rho_{eq}(J_s)] \right\}^{-1} . \quad (3.25)$$

This *internal* energy diffusion rate constant depends upon

TABLE II. Dissociation rate constants, divided by $\zeta e^{-\beta E_d}$, for the harmonic and Morse oscillator models.

	βE_d	κ_f [a]	k_f [b]	k_f^{num} [c]	κ_f^{Krd} [d]
(HO)	2	3.7	2.4	2.4	2.0
	5	4.8	4.2	4.1	5.0
	10	9.1	8.9	8.9	10.0
(MO)	2	4.5	2.7	2.8	4.0
	5	6.4	5.4	5.1	10.0
	10	13.2	13.0	12.9	20.0

[a]Calculated from Eq. (3.22).
[b]Calculated from Eq. (3.26).
[c]From Ref. 39.
[d]Calculated from Eq. (3.20).

the approach of the distribution $\rho^0(J_s, t|J_s)$ at J_s to its equilibrium value if $J=J_s$ initially and no reaction is allowed. The total dissociation rate constant is then [cf. Eq. (1.4)]

$$k_f=(1+\kappa_f/\kappa_R)^{-1}\kappa_f \ . \tag{3.26}$$

The tcf expression (3.25) for κ_R is approximately evaluated in Appendix B as

$$\kappa_R^{-1}=\int_0^{J_s} dJ\, e^{-\beta E(J)} \int_0^J dJ' R(J') \ . \tag{3.27}$$

Thus, κ_R^{-1} is a weighted and integrated resistance to energy flow up to J_s, the upper boundary of the stable state.

Our numerical results for the HO and MO are given in Table II. Aside from the excellent agreement with the results of Bak and Andersen,[39] the main point of Table II is the following: For small βE_d, κ_f begins to severely overestimate the rate, due to the neglect of the slow energy equilibration, governed by κ_R, in the stable state. This energy flow is not slow enough to be rate limiting in the overall flow to E_d, but does exert an important influence. (When $\beta E_d=2$, $\kappa_f/\kappa_R\approx 0.6$; internal energy relaxation is only about twice as fast as flow through I. In contrast, $\kappa_f/\kappa_R\approx 10^2$ when $\beta E_d=10$.) The SSP equation (3.26) correctly accounts for this effect.

4. *Alternate stable state definition*

An important characteristic of the SSP is its flexibility. In the preceding subsections, we have defined the reactant stable state by energies $0\le E\le E_s$ such that internal equilibrium applied when $\beta E_d\gg 1$. Suppose that we *redefine* the stable state to be the entire energy range from zero up to the dissociation energy E_d. Then the discussion of Appendix E of I and Eq. (1.4) show that we can write the rate constant as

$$k_f=(\kappa_f^u+\kappa_{R'})^{-1}\kappa_{R'}\kappa_f^u \ . \tag{3.28}$$

Here κ_f^u is the rate constant for the rapid dissociative step at E_d and [cf. Eq. (3.25)]

$$\kappa_{R'}=\kappa_R(J_s\to J_d) \tag{3.29}$$

is just the internal energy diffusion rate constant for the entire stable state $0\le E\le E_d$. Since the model prescription of Sec. III B 1 tells us that $\kappa_f^u\gg\kappa_{R'}$, Eq. (3.29) simplifies. We can find the rate constant $k_f=\kappa_{R'}$ by evaluating $\kappa_{R'}$, i.e., by letting $J_s\,J_d$ in Eq. (3.27) for κ_R. We have then[41,42]

$$k_f=\left[\int_0^{J_d} dJ\, e^{-\beta E(J)} \int_0^J dJ' R(J')\right]^{-1} \ . \tag{3.30}$$

In this version of the SSP, the entire rate constant is determined by nonequilibrium energy flow *within* the stable state R'. This is, of course, a consequence of our definition of R' to include both R and the intermediate region I.

For both oscillator cases, shown in Table I, the agreement of Eq. (3.30) with our previous stable states result κ_f is excellent. Indeed, examination of the dominant contributions to Eq. (3.22) shows that, for $\beta E_d\gg 1$,[43]

$$k_f\approx\kappa_f=\left[\int_0^{J_d} dJ\, e^{-\beta E(J)} \int_0^J dJ' R(J')\right]^{-1} \ . \tag{3.31}$$

As in Eq. (3.27), this involves the equilibrium average of the integrated resistance to energy flow.

C. Generalizations

The results presented above can be generalized in several directions. We begin with the diffusion-controled regime (Sec. III B). First, unimolecular dissociation need not always be rapid compared to internal energy diffusion, especially at higher buffer gas densities. If κ_f^u denotes the intrinsic unimolecular rate constant for this dissociation at E_d, then the overall rate constant is [cf. Eq. (1.4)]

$$k_f^{-1}=(\kappa_f^u)^{-1}+\kappa_f^{-1} \ , \tag{3.32}$$

where κ_f is given by either Eqs. (3.22), (3.30), or (3.31) if $\beta E_d\gg 1$.

Second, if the reaction is a reversible isomerization (Fig. 5), then the overall rate constant is [cf. Eq. (1.5) and Sec. IV or I]

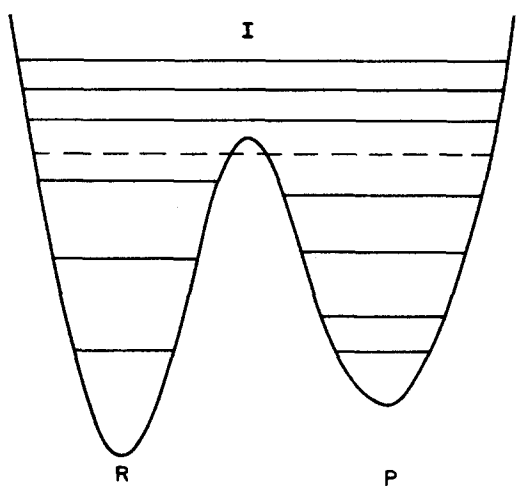

FIG. 5. Schematic potential energy and level diagram for an isomerization. The reaction coordinate is unspecified but might, for example, correspond to an angle. Only a few levels are shown. Note that the levels above the barrier top are properly included in region I. With reference to Eq. (3.36), E_p is the minimum product energy and E_0 is the lowest I region energy.

$$k_f = [1 + (\kappa_f^u/\kappa_R) + (\kappa_r^u/\kappa_P)]^{-1}\kappa_f^u \ . \tag{3.33}$$

Here κ_R and κ_P are the internal rate constants for the reactant and product; κ_f^u and κ_r^u are the intrinsic forward and reverse unimolecular rate constants for intramolecular interconversion at threshold, respectively. Equation (3.33) shows the characteristic dependence on *both* forward and reverse reactive processes discussed at length in I. In the low density limit, κ_f^u and κ_r^u greatly exceed κ_R and κ_P, respectively. Then κ_f is determined only by κ_R, κ_P, and the equilibrium constant $K^{eq} = \kappa_f^u/\kappa_r^u$. If the isomerization double well potential is symmetric, then $K^{eq} = 1$ and[1,3,4]

$$k_f^{-1} = \kappa_R^{-1} + \kappa_P^{-1} = 2\kappa_R^{-1} \ . \tag{3.34}$$

Thus, k_f is reduced by a factor of 2 compared to the reactant rate constant κ_R. The physical origin of this reduction is simple: The rate is determined by slow activation up to the threshold *and* slow deactivation down into the product well.[1,3,4]

We limit our comments on the strong coupling case (Sec. III A) to the generalization to an isomerization in the low density limit. Then, for example, Eq. (3.13) is replaced by

$$k_f^{-1} = \kappa_f^{-1} + (K^{eq}\kappa_r)^{-1} \ , \tag{3.35}$$

where κ_r is the reverse rate constant (cf. Fig. 5)

$$\kappa_r = \int_{E_P}^{E_0} d\epsilon\, \rho_P^{eq}(\epsilon) \int_{\epsilon}^{\infty} d\epsilon' K(\epsilon - \epsilon') \tag{3.36}$$

and K^{eq} is the equilibrium constant. The importance of stable product formation is again emphasized by Eq. (3.35). At low density, the forward rate is determined not by passage back and forth at energy E_0 between the well "tops" but by promotion out of the reactant well *and* stabilization in the product well (Fig. 5).

Finally, we have considered sensible but simplified models of the dynamics in both the strong and weak coupling limits. It is possible (and important) to apply our SSP formulas for more complex and realistic dynamical models.[25,27,33] Our current efforts[12] are focused on rate constants for "sticking" on the surfaces of solids[34(b)] and gas phase clusters.[29]

IV. REACTIONS IN SOLUTION: BARRIER CROSSING MODELS

We now apply the SSP and our rate constant formulas to models of chemical reactions in liquids. We will focus on the reaction viewed as passage over a mean potential barrier between two wells. The classic investigation of Kramers[32] still provides a standard reference point for this problem. We therefore briefly review some salient aspects of Kramers' approach and results.

Kramers viewed the (forward) reaction as a one dimensional passage of an effective "particle" over a potential barrier located between reactant and product potential wells. This motion was described by the stochastic Langevin equation (LE)

$$\mu\, dv/dt = F - \zeta v + F^* \tag{4.1}$$

for the acceleration of the particle of mass μ. The force arising from the potential is F; F^* is a Gaussian random force.[44] The net effect of the "collisions," i.e., dynamical interactions, between particle and solvent is thus approximately accounted for by the frictional or damping force $F_d = -\zeta v$, where ζ is a friction constant. The potential in the barrier region was taken as an inverted parabola with a frequency ω_b related to the barrier curvature $|k_b|$ by $\omega_b = (|k_b|/\mu)^{1/2}$.

Kramers analyzed the steady state Fokker–Planck equation associated with the LE (4.1) to find the rate constant[2,32,45]

$$\kappa^{Kr} = \kappa^{TST}\{[(\zeta/2\mu\omega_b)^2 + 1]^{1/2} - (\zeta/2\mu\omega_b)\} \ . \tag{4.2}$$

(In this section, we drop the subscript f denoting "forward.") Kramers' result κ^{Kr} predicts a reduction, due to collisions, of the rate constant from its TST value

$$\kappa^{TST} = (\omega_R/2\pi)\, e^{-\beta E_0} \ . \tag{4.3}$$

Here ω_R is the frequency of the reactant well bottom and E_0 is the activation energy ($\beta E_0 \gg 1$). This TST result is, in turn, based on *two* key assumptions:

(a) full internal equilibrium holds on the *entire* reactant side of the barrier for particles passing to products and

(b) each and every passage across the barrier top maximum leads to products without an intervening recrossing, i.e., free or inertial streaming holds across the barrier top.

In fact, Kramers' result shows that collisions occurring in the barrier *region* lead to at least a partial, and sometimes an extreme, breakdown of both assumptions. Thus, at low and intermediate friction ($\zeta/\omega_b\mu \ll 1$), intercepting collisions can return a particle to the reactant side of the barrier before recognizable product is formed. Under high friction conditions ($\zeta/\omega_b\mu \gg 1$), continuous collisional buffeting leads to repeated barrier top crossing and recrossing. The memory, or correlation, time $(\zeta/\mu)^{-1}$ of the particle's directed velocity is short compared to the time spent on or near the barrier top. Here velocity equilibrium applies but there is significant *spatial* nonequilibrium. Then $\kappa^{Kr} \propto \zeta^{-1}$, thus characterizing a "diffusion-controlled" passage across the barrier region.

Two central assumptions made by Kramers in finding Eq. (4.2) are of major importance. These are[32] (a) internal equilibrium holds "near" the well bottom associated with the reactants, i.e., *away* from the barrier top; (b) at some point *past* the barrier top, passage into the product well is essentially certain. (Note the difference between these and the TST assumptions.)

The above two assumptions coincide precisely with those of our SSP (cf. Sec. I). Indeed, Northrup and Hynes[2] obtained Kramers' equation (4.2) by evaluation of a Green's function version of the tcf expression for the SSP barrier rate constant [cf. Eq. (1.1)]

$$\kappa = \int_0^{\infty} dt\, \langle j_i(S_R) j_o^*(S_P, t)\rangle_R \ . \tag{4.4}$$

We now discuss the evaluation of Eq. (4.4) for more realistic models of the dynamics.

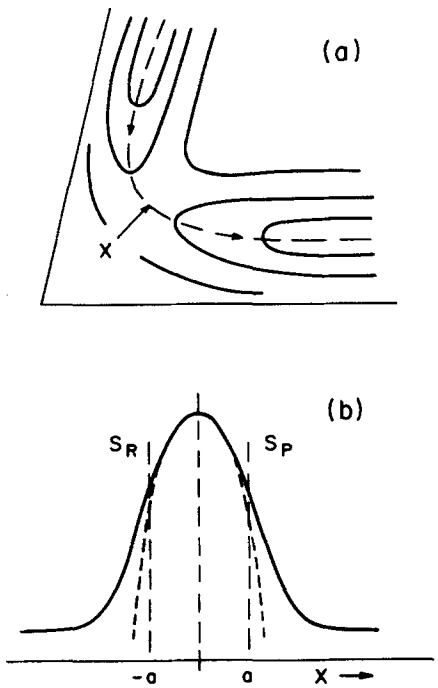

FIG. 6. Schematic model for barrier crossing reactions in solution. (a) *Mean* potential energy surface indicating the reaction coordinate x. Solvent collisions lead to various motions on this surface not dictated exclusively by the surface itself. (b) One dimensional cut along x indicating the stable state dividing surfaces. The extended potential is shown (- - -) (see the text). For an isomerization, there would be potential wells in the stable reactant and product regions.

A. Model for barrier crossing

Our model for solution reactions is shown in Fig. 6(a). The "reaction coordinate" (a) leads from reactants to products and (b) passes through a saddle point region. This picture would apply, for example, to atom transfer reactions[23,46(a)] or structural isomerizations.[23,46] We next isolate this reaction coordinate and reduce the problem to motion of some effective particle of mass μ in the one dimensional potential of Fig. 6(b). (This step is made for simplicity; as discussed in Sec. IV E, it need not be taken.)

In the SSP, the stable reactant and product state surfaces are located *away* from the barrier top. These and the intermediate or barrier region I are shown in Fig. 6(b). We make the SSP assumptions that the continual interactions with solvent molecules are sufficient (a) to maintain internal equilibrium in the reactants R and (b) to stabilize incipient products P so that passage through S_P is irreversible on the time scale that determines the rate constant. By conservative estimate (see below), these conditions will hold for activation energies $\beta E_0 \gtrsim 5$. Then the rate constant is given by Eq. (4.4).

We must now specify a model for the dynamics along the reaction coordinate in the presence of the solvent. We assume that a *generalized* Langevin equation (GLE)

$$\mu \frac{dv}{dt}(t) = F(t) - \int_0^t d\tau \zeta(\tau) v(t-\tau) + F^*(t) \tag{4.5}$$

holds in the intermediate, or barrier, region.[47] We also assume that the static potential is an inverted parabola in this region so that

$$F = \mu \omega_b^2 x \ . \tag{4.6}$$

The time dependent friction $\zeta(t)$ is the solvent-averaged tcf of the fluctuating forces exerted on the effective particle along the reaction coordinate

$$\zeta(t) = \beta \overline{F^*F^*(t)} \ . \tag{4.7}$$

We assume that $F^*(t)$ is a *Gaussian* random force.[44] These fluctuating forces arise only from the dynamical interaction with the solvent; any average or mean solvent potential forces are accounted for by F.[48] In the simplest case where the reaction coordinate x is a relative spatial or angle difference, F^* is to be computed along this coordinate. In an atom-transfer reaction A + BC $\rightarrow$ AB + C, F^* is along a combination of vibrational normal coordinates.[24,46] In any event, the tcf $\zeta(t)$ associated with the barrier region I will generally be *quite different* from that appropriate in the reactant and product regions. We will determine κ for any given $\zeta(t)$ and then examine a few representative models of $\zeta(t)$.

The non-Markovian GLE (4.5) reduces to the Markovian LE (4.1) *if* the random force correlations decay rapidly while the velocity hardly changes. Then

$$\int_0^t d\tau \zeta(\tau) v(t-\tau) \approx \zeta v(t) \tag{4.8}$$

and the friction only enters through the "zero-frequency" component

$$\zeta = \hat{\zeta}(0) = \int_0^\infty dt \zeta(t) \tag{4.9}$$

of the Laplace transform $\hat{\zeta}(\epsilon) = \int_0^\infty dt\, e^{-\epsilon t} \zeta(t)$ of the time dependent friction $\zeta(t)$. This reduction (GLE $\rightarrow$ LE) is usually a very *poor* approximation. For *single* molecule motion in liquids, it completely misses important velocity correlation features such as "caging."[49] It is, however, often argued that the LE is satisfactory for reactions. Supposedly, information is required only on long time scales of order $\kappa^{-1} \propto e^{\beta E_0}$; short time details such as those incorporated in $\zeta(t)$ are presumed to be irrelevant.

The (incorrect) argument just given misses the essential point: Dynamics that determine κ are often associated with *high frequency* motion in the barrier region where strong forces operate. Consider, for example, passage over a typically sharp, high frequency (ω_b) barrier when the friction is not too high. The barrier crossing rate for a particle will depend upon the short time "nonadiabatic" friction experienced *during* the passage and will involve high frequency components $\hat{\zeta}(\epsilon)$ of the spectral resolution of $\zeta(t)$. The successful passage to stable product can be made long *before* the "adiabatic" approximation (4.8) holds; the GLE must be retained.

Our argument above has been simplified for emphasis. Its major point, i.e., that κ should depend on the details of the dynamics reflected in $\zeta(t)$, will be verified below.

B. Rate constant evaluation

1. Simplification

The tcf in Eq. (4.4) for κ can be considerably simplified by the following device to replace the BC's at $S_R = -a$ and $S_P = a$[4]: The true potential is artificially extended beyond $-a$ and a [Fig. 6(b)]. These artificial forces play the same role as the BC's in providing essentially complete absorption past $-a$ and a. Now, however, we can accurately use *unrestricted* dynamics on the full extended potential.[50,51]

With the above replacement, we need not require solely incoming and outgoing fluxes at $S_R = -a$ and $S_P = a$, respectively. The dynamics itself will take care of this; any recrossing trajectories will cancel their own contribution. Therefore we can write the rate constant as[50,51]

$$\kappa = \int_0^\infty dt \langle j(S_R) j(S_P, t) \rangle_R \ . \tag{4.10}$$

Many alternate forms of Eq. (4.10) analogous to those of Sec. II could be used in the following; they all will yield the same result.[51]

2. Time-dependent probability density

We begin the evaluation of Eq. (4.10) by writing out the integrand in terms of the probability distribution $\rho(x, v, t|x_0, v_0)$. This governs the "particle's" position x (with respect to the barrier top) and velocity v at time t, given the initial values x_0 and v_0. We obtain

$$\kappa = \int_0^\infty dt \int dx\, dv \int dx_0 dv_0 \phi_{eq}(v_0)\psi_{eq}(x_0) \times v_0 \delta(x_0 + a) v \delta(x - a) \rho(x, v, t|x_0, v_0) \ , \tag{4.11}$$

which simplifies to

$$\kappa = \psi_{eq}(-a) \int_0^\infty dt \int dv_0 \times \int dv \phi_{eq}(v_0) v_0 v \rho(a, v, t|-a, v_0) \ . \tag{4.12}$$

Here $\phi_{eq}(v)$ is the Maxwellian and

$$\psi_{eq}(-a) = e^{-\beta U(-a)}/Q_R = e^{-\beta E_0} \exp[\beta(\mu\omega_b^2/2)a^2]/Q_R \tag{4.13}$$

is the equilibrium probability for $x = -a$. The activation energy is E_0.

Since the "random" force in the GLE (4.5) is assumed to be Gaussian, the probability distribution of relative positions and velocities at time t is *also* Gaussian[44,52]:

$$\rho(x, v, t|x_0, v_0) = \pi^{-1} |\det \mathbf{Q}^{-1}|^{1/2} \exp(-\mathbf{y}^T \cdot \mathbf{Q}^{-1} \cdot \mathbf{y}) \ . \tag{4.14}$$

The vector $\mathbf{y}$ represents the fluctuations in x and v from their (time-dependent) average values:

$$y_1 = x - \bar{x}^{x_0, v_0}(t) \ , \quad y_2 = v - \bar{v}^{x_0, v_0}(t) \ . \tag{4.15}$$

The matrix $\mathbf{Q}$ is proportional to the second moments of the distribution:

$$Q_{ij}(t) = 2\overline{y_i y_j}^{x_0, v_0}(t) \ . \tag{4.16}$$

We will require explicit expressions for the average displacement $\bar{x}^{x_0, v_0}(t)$ and velocity $\bar{v}^{x_0, v_0}(t)$. By formally solving the GLE (4.5) by Laplace transformation as an initial value problem and noting that the average $\overline{F^*}^{x_0, v_0}(t)$ vanishes, we find that

$$\bar{x}^{x_0, v_0}(t) = C_{11}(t)x_0 + C_{12}(t)v_0 \ , \tag{4.17a}$$

$$\bar{v}^{x_0, v_0}(t) = C_{21}(t)x_0 + C_{22}(t)v_0 \ . \tag{4.17b}$$

The time dependent coefficients $C_{ij}(t)$ are found to be related to one of them $[C_{21}(t) \equiv C(t)]$ according to

$$\dot{C}_{11} = C(t) \ , \quad \dot{C}_{12} = C_{22}(t) \ , \quad \dot{C}(t) = \omega_b^2 C_{22}(t) \ , \tag{4.18a}$$

with initial values $C_{11}(0) = 1$, $C_{12}(0) = 0$, $C_{21}(0) = 0$, and $C_{22}(0) = 1$.

According to Eq. (4.17b) the coefficient $C_{21}(t) = C(t)$ determines the average velocity at time t if the particle starts at rest at position x_0 with respect to the barrier top:

$$C(t) = \bar{v}^{x_0, 0}(t)/x_0 \ . \tag{4.18b}$$

The formal solution to this initial value problem shows that the Laplace transform of $C(t)$ is

$$\hat{C}(\epsilon) = \omega_b^2[\epsilon^2 - \omega_b^2 + \epsilon\mu^{-1}\hat{\zeta}(\epsilon)]^{-1} \ . \tag{4.19}$$

Here the frequency-dependent friction is the transform

$$\hat{\zeta}(\epsilon) = \int_0^\infty dt\, e^{-\epsilon t}\zeta(t) \tag{4.20}$$

of the time dependent friction.

3. Reactive frequency and κ

The time dependence of $C(t)$ [Eq. (4.18)] has one special feature crucial to our development: There is a positive reactive eigenvalue, or frequency, in its spectrum. This frequency arises from the *unstable*, or divergent, motion in the barrier region. Therefore, the reactive frequency exclusively governs the long time behavior of $C(t)$. To see this, consider first the case of no friction. Then, according to Eq. (4.19), we have

$$C(t) = (\omega_b/2)(e^{\omega_b t} - e^{-\omega_b t}) \ . \tag{4.21}$$

In this trivial case, the actual barrier frequency ω_b in the diverging exponential is the reactive frequency or eigenvalue. In the general case when friction is present, we can formally represent $C(t)$ as

$$C(t) = \sum_n C_n e^{-\lambda_n t} + C_r e^{\lambda_r t} \ . \tag{4.22}$$

The frequencies $\lambda_n > 0$ govern modes of stable relaxation which need not concern us here. *The positive reactive frequency (eigenvalue) λ_r reflects the unstable reactive motion in the barrier region.*[53]

Our concern with λ_r will now be justified. According to our tcf formula (4.12) and the distribution (4.14), the rate constant κ is

$$\kappa = \psi_{eq}(-a) \int_0^\infty dt \int dv \int dv_0 \phi_{eq}(v_0) v_0 v \pi^{-1} \times |\det Q(t)|^{-1/2} \exp[-\mathbf{y}^T(t) \cdot \mathbf{Q}^{-1}(t) \cdot \mathbf{y}(t)] \ , \tag{4.23}$$

where $x_0 = -a$ and $x = a$ are to be taken. In Appendix C,

this formidable expression is exactly evaluated to give the exceedingly simple result

$$\kappa = \kappa^{\mathrm{TST}}(\lambda_r/\omega_b) \ . \tag{4.24}$$

Thus, the rate constant is just the TST rate constant

$$\kappa^{\mathrm{TST}} = [(2\pi\beta\mu)^{1/2} Q_R]^{-1} e^{-\beta E_0} = (\omega_R/2\pi)\, e^{-\beta E_0} \tag{4.25}$$

times the ratio of the reactive frequency λ_r and the barrier frequency ω_b.

To determine the reactive frequency λ_r, we consider Eq. (4.19) in time language

$$\partial C(t)/\partial t = \omega_b^2 \pi(t) + \omega_b^2 \int_0^t d\tau \pi(\tau) C(t-\tau) \ , \tag{4.26}$$

where $\pi(t)$ is the inverse transform of $\hat{\pi}(\epsilon) = [\epsilon + \hat{\zeta}(\epsilon)/\mu]^{-1}$. We can find λ_r if we look for a long time solution $C(t) \sim C_r e^{\lambda_r t}$. Substitution into Eq. (4.26) and passage to the long time limit gives [$\pi(t) \to 0$ as $t \to \infty$]

$$\lambda_r = \omega_b^2 \int_0^\infty d\tau\, e^{-\lambda_r \tau} \pi(\tau) \ . \tag{4.27}$$

Since $\hat{\pi}(\epsilon) = [\epsilon + \hat{\zeta}(\epsilon)/\mu]^{-1}$, this gives our desired result

$$\lambda_r = \frac{\omega_b^2}{\lambda_r + \hat{\zeta}(\lambda_r)/\mu} \ . \tag{4.28}$$

We will therefore generally need to know the behavior of $\zeta(t)$ at *all* times through $\hat{\zeta}(\lambda_r)$; our long time limit was only a method of extracting Eq. (4.28).

C. Discussion of the rate constant

Equations (4.24) and (4.28) are our key results. They show that (a) κ is determined by λ_r and that (b) the reactive frequency λ_r is determined both by the barrier frequency ω_b and by the frequency component of the time dependent friction

$$\hat{\zeta}(\lambda_r) = \int_0^\infty dt\, e^{-\lambda_r t} \zeta(t) \tag{4.29}$$

at the reactive frequency λ_r.

The self-consistent equation (4.28) for λ_r can be written in an instructive form when we realize that

$$\hat{\pi}(\epsilon) = [\epsilon + \hat{\zeta}(\epsilon)/\mu]^{-1} \tag{4.30}$$

is the Laplace transform of the velocity tcf[49]

$$\pi(t) = \langle v^2 \rangle^{-1} \langle v v(t) \rangle \tag{4.31}$$

for the motion of a hypothetical particle of mass μ obeying the GLE

$$\mu\, dv(t)/dt = -\int_0^t d\tau \zeta(\tau) v(t-\tau) + F^*(t) \tag{4.32}$$

in the *absence* of the barrier, but experiencing the actual friction. Thus, Eq. (4.28) can be written as

$$\lambda_r = \omega_b^2 \int_0^\infty dt\, e^{-\lambda_r t} \langle v^2 \rangle^{-1} \langle v v(t) \rangle$$

$$= \omega_b^2 \int_0^\infty dt\, e^{-\lambda_r t} \pi(t) \ . \tag{4.33}$$

Many qualitative aspects of the rate constant κ follow from Eq. (4.33). If the friction is very *weak* [$\hat{\zeta}(\lambda_r)/\mu \ll \lambda_r$], the velocity correlations die very slowly compared to $e^{-\lambda_r t}$. Trajectories across the barrier are negligibly perturbed by collisions with solvent molecules [cf. Fig. 7(a)] and Eq. (4.33) gives

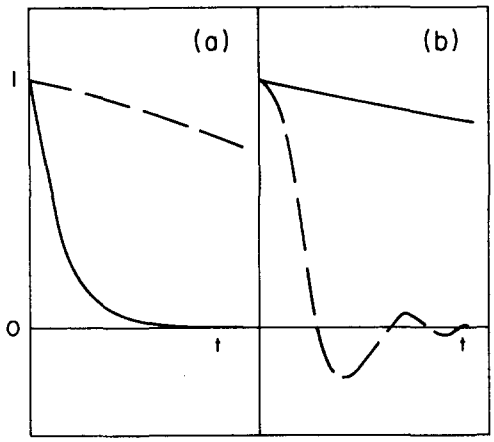

FIG. 7. Illustration of the time behavior of $\exp(-\lambda_r t)$ (—) and the velocity tcf $\pi(t)$ (- - -) in the cases of (a) low friction and (b) high friction.

$$\lambda_r \approx \omega_b^2 \int_0^\infty dt\, e^{-\lambda_r t} \pi(t=0) = \omega_b^2/\lambda_r \tag{4.34}$$

or $\lambda_r \cong \omega_b$. Thus, the reactive frequency is just the barrier frequency and the TST result (4.25) is obtained.

In the opposite limit of *large* friction [$\hat{\zeta}(\lambda_r)/\mu \gg \lambda_r$], barrier region trajectories are strongly and continually perturbed by solvent collisions. The reactive frequency will then be much less than ω_b; "shuttling" back and forth across the barrier top occurs before final stabilization in either the reactant or product stable states [cf. Fig. 7(b)]. Velocity correlation, or memory, dies rapidly compared to $e^{-\lambda_r t}$ and Eq. (4.33) gives

$$\lambda_r \approx \omega_b^2 \int_0^\infty dt\, \pi(t) = \mu\omega_b^2/\hat{\zeta}(0) \ . \tag{4.35}$$

We thus obtain the *diffusion limit* result of Kramers[4,32]

$$\kappa/\kappa^{\mathrm{TST}} = \mu\omega_b/\zeta \ , \tag{4.36}$$

which is inversely proportional to the zero-frequency, or steady state, friction $\hat{\zeta}(0) = \zeta$. This is the only limit in which the friction *constant* provides a satisfactory description of the interaction with the solvent. In general, we require a knowledge of the full dynamics in $\zeta(t)$. We consider this next.

D. Influence of time-dependent friction

We now examine our rate constant result [Eqs. (4.24) and (4.28)] for several interesting models of the time dependent friction $\zeta(t)$ in the barrier region. For purposes of comparison, we begin with the Kramers assumption.

1. *Delta friction*

The reduction of the GLE to the LE with constant friction is equivalent to the delta function assumption

$$\zeta(t) = \zeta\delta(t) \ . \tag{4.37}$$

Thus, the full force of the integrated friction $\zeta = \int_0^\infty dt \zeta(t)$ is effective instantaneously. This gives $\hat{\zeta}(\lambda_r)$

$=\zeta$ and $\lambda_r=\{[(\zeta/2\mu\omega_b)^2+1]^{1/2}-(\zeta/2\mu\omega_b)\}\omega_b$ from Eq. (4.28). Since $\kappa=\kappa^{TST}(\lambda_r/\omega_b)$, this yields the Kramers result (4.2).

2. Gaussian friction

A reasonable model for $\zeta(t)$ for short and intermediate times is the Gaussian

$$\zeta(t)=\zeta_0 e^{-\gamma^2 t^2} . \tag{4.38}$$

This form can give an oscillatory velocity tcf (4.31), i.e., aspects of dense fluid "caging" of the velocity.[49] The required transform $\hat{\zeta}(\lambda_r)$ is

$$\hat{\zeta}(\lambda_r)=\zeta \exp(\lambda_r/\gamma)^2 \operatorname{erfc}(\lambda_r/\gamma) ; \tag{4.39}$$

erfc is the complementary error function and $\zeta=\zeta_0\sqrt{\pi}/\gamma$ is the zero frequency friction. With Eq. (4.39) for $\hat{\zeta}(\lambda_r)$, Eq. (4.28) can be solved numerically to determine λ_r; this then gives the rate constant by Eq. (4.24).

Our results are shown in Fig. 8 for representative values of the key parameter γ/ω_b, the ratio of the friction decay rate to the barrier frequency. Except for broad barriers, reasonable estimates give γ/ω_b values of 0(1) or less. The effective friction $\hat{\zeta}(\lambda_r)$ can then be dramatically less than the zero frequency value ζ. When, for example, $\omega_b \approx 10^{14}$ sec^{-1} and $\gamma \approx 10^{13}$ sec^{-1}, the effective friction is quite low; κ is very close to its TST value. This suggests very strongly that many solution phase rate constants will be well approximated by the TST prediction; the constant friction approximation κ^{Kr} can often *drastically* overestimate the solvent's influence. As is evident from Fig. 8 , this overestimate becomes less severe as the barrier becomes broader.

3. Oscillatory friction

Our final model friction is oscillatory in time:

$$\zeta(t)=\zeta_0 e^{-\gamma t/2}[\cos(\omega_1 t)+(\gamma/2\omega_1)\sin(\omega_1 t)] . \tag{4.40}$$

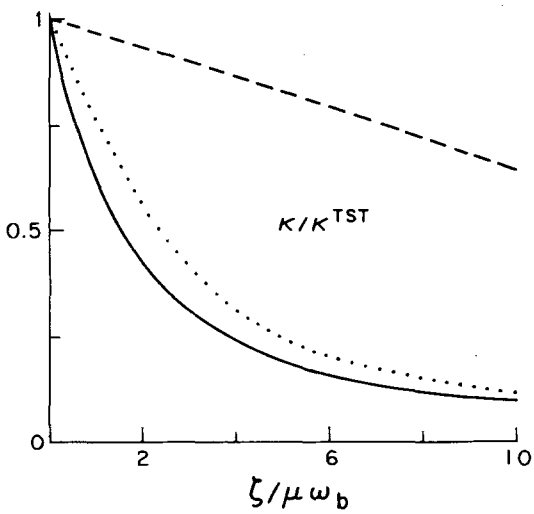

FIG. 8. Ratio κ/κ^{TST} of the rate constant to its transition state value, for the Gaussian friction model. The reduced zero frequency friction is $\zeta/\mu\omega_b$. Legend: (—), zero frequency friction result Eq. (4.2); (•••), $\gamma/\omega_b=1.0$; (- - -), $\gamma/\omega_b=0.1$. [As ζ approaches 0, κ should approach zero; the SSP in energy space space should be used instead. This behavior is limited to the extremely small ζ region on our scale (Sec. IV. E).]

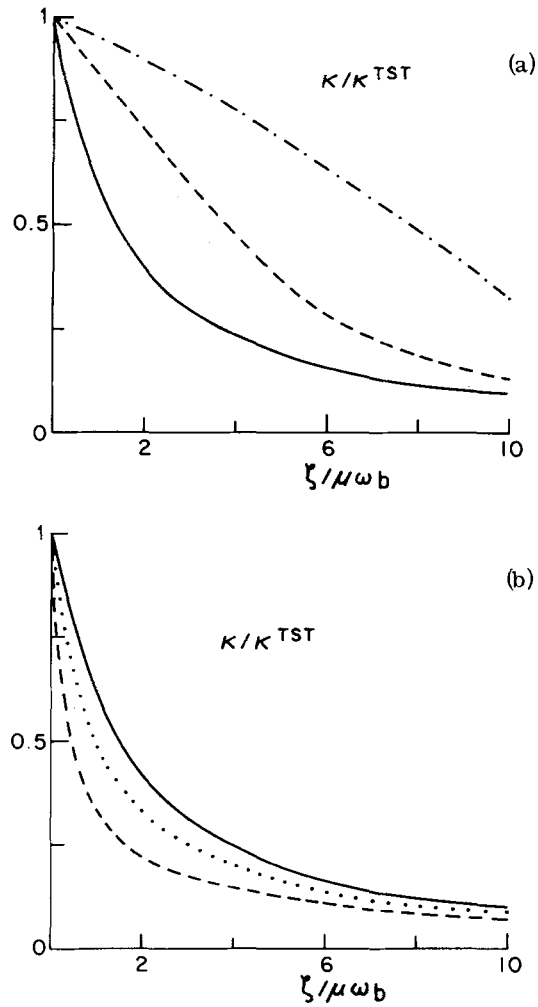

FIG. 9. Ratio κ/κ^{TST} of the rate constant to its transition state value, for the oscillatory friction model, versus reduced zero frequency friction. (a) $\omega_1/\omega_b=0.1$; (— —), $\omega_1/\gamma=0.5$; (- - -), $\omega_1/\gamma=0.1$. (b) $\omega_1/\omega_b=10.0$; (•••), $\omega_1/\gamma=10$; (- - -), $\omega_1/\gamma=50$. In both (a) and (b), the solid line is the zero frequency friction result (4.2), which is independent of ω_1/ω_b and ω_1/γ at fixed reduced friction.

Here γ measures the overall decay rate and ω_1 gauges the oscillatory behavior. This model appears sensible when the solvent is solid[54(a)] or very strong forces (e.g., electrostatic) restrict the solvent molecules.[54(b)] The required transform is

$$\hat{\zeta}(\lambda_r)=\zeta_0(\gamma+\lambda_r)[\omega_1^2+(\lambda_r+\tfrac{1}{2}\gamma)^2]^{-1} \tag{4.41}$$

and the zero frequency value is $\zeta=4\zeta_0\gamma/(\gamma^2+4\omega_1^2)$.

The results for κ shown in Fig. 9 display an interesting variety. In Fig. 9(a), the barrier frequency ω_b exceeds the oscillatory frequency ω_1 of the friction. The oscillations in $\zeta(t)$ are largely irrelevant; they do not develop before successful barrier passage occurs. In all cases, $\zeta=\hat{\zeta}(0)$ is a significant overestimate of the effective friction and $\kappa>\kappa^{Kr}$, as in the Gaussian case.

The opposite limit where $\zeta(t)$ oscillates on a time scale fast compared to a (broad) barrier frequency is shown in Fig. 9(b). $\hat{\zeta}(\lambda_r)$ can be much *greater* than $\hat{\zeta}(0)$; κ rapidly drops below both κ^{TST} *and* κ^{Kr}. This behavior

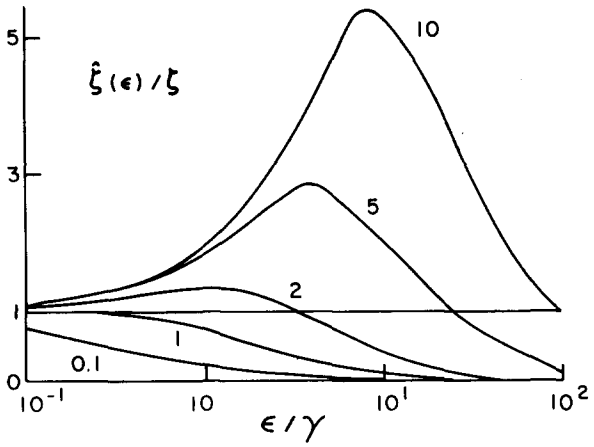

FIG. 10. Ratio $\hat{\zeta}(\epsilon)/\zeta$ of the frequency dependent friction to its zero frequency value ζ in the oscillatory friction case versus reduced frequency ϵ/γ. Values of the parameter ω_1/γ are indicated.

is most easily explained via Fig. 10, which gives the frequency dependence of $\hat{\zeta}(\epsilon)$. When ω_1/ω_b is large, there is a significant range of high frequencies $\epsilon \approx \omega_1$ where $\hat{\zeta}(\epsilon)$ far exceeds ζ; at low frequencies, integrated oscillations cancel and lead to a low friction value. If the oscillations are weakly damped, the enhanced friction effect is pronounced and a dramatic reduction in κ versus $\zeta/\mu\omega_b$ results. Note that this depression of κ occurs for *slow* damping of $\zeta(t)$; this is just the *opposite* of the usual Markovian assumption $\zeta(t) = \zeta\delta(t)$.

4. Some generalities

The above results show that the *details* of the time dependent friction play a significant role in the magnitude of the rate constant. This makes generalizations dangerous, but a few can be stated. First, Eqs. (4.24) and (4.28) tell us that if $\hat{\zeta}(\lambda_r) < \zeta$, then $\kappa > \kappa^{Kr}$; if $\hat{\zeta}(\lambda_r) > \zeta$, then $\kappa < \kappa^{Kr}$. The oscillatory $\zeta(t)$ example, however, shows that a transition between these regimes can occur. Finally, in a number of cases the friction can likely be adequately represented as

$$\zeta(t) = \zeta_f(t) + \zeta_s(t) , \tag{4.42}$$

i.e., a combination of fast (on the scale of ω_b^{-1}) and more slowly varying contributions. Then $\hat{\zeta}(\lambda_r) \approx \hat{\zeta}_f(0) + \hat{\zeta}_s(\lambda_r)$ determines the rate constant κ, whose value will typically lie *between* the values predicted by assuming either $\hat{\zeta}(\lambda_r) \approx \hat{\zeta}_f(0)$ or $\hat{\zeta}(\lambda_r) \approx \hat{\zeta}_f(0) + \hat{\zeta}_s(0)$. Clearly, the time dependent friction $\zeta(t)$ in barrier regions deserves extensive study.

E. Extensions and limitations

There is no real need to restrict the derivation of Eq. (4.24) for κ to one dimension ($1D$). Suppose that degrees of freedom perpendicular to the reaction coordinate (cf. Sec. IV A) *remain* in equilibrium throughout the barrier passage. Then Eq. (4.4) can be extended to $3D$ by including in κ^{TST} certain well known equilibrium factors related to saddle point and reactant well harmonic frequencies.[55] In general, however, dynamic coupling drives the perpendicular degrees of freedom *out* of equilibrium during the passage.[11,46] Fortunately, this can be accounted for in Eq. (4.5) by inclusion of the coupling effects in the friction $\zeta(t)$. This will be discussed elsewhere for atom-transfer reactions and structural isomerizations.[46]

We have only examined very simple models for the friction $\zeta(t)$. One can clearly do a better job by analysis of suitable molecular expressions for $\zeta(t)$.[48,56] Furthermore, in addition to the "internal" couplings mentioned above, couplings to appropriate time scale relaxation phenomena in the *solvent* can influence $\zeta(t)$. Thus, dielectric[57] and ionic[58] relaxation can influence reactions involving ionic and/or dipolar species[59] in solution. These are currently under study.

An important concern is the validity of our Gaussian assumption (GA) [Eq. (4.14)]. This is difficult to establish precisely. Some favorable evidence is available for *single* molecule motion in dense fluids. First, the GA is exact for short times[60(a)] and harmonic forces.[60(b)] Second, the GA gives a satisfactory account for a wide range of dynamical quantities. These include atomic position correlations,[60(c)] correlations of molecular linear and angular velocity,[60(d)] and possibly internal angular motion in protein models.[60(e)] For motion in barrier regions, we believe that the GA remains reasonable. A likely exception is the motion of a very light effective particle surrounded by massive solvent molecules, a situation recently modeled by Skinner and Wolynes.[31] Finally, the GA only holds for massive particles in light solvents *if* the interactions are modeled as impulsive, e.g., hard sphere collisions.[60(f)] Real forces are continuous, however. Their legitimate approximation as impulsive forces remains to be established for reaction problems where high frequency phenomena are often involved (as in vibrational energy transfer[24(a)]). Our results suggest that this approximation should only be used with caution.

The SSP internal equilibrium assumption discussed in Sec. IV A may break down under certain conditions. For *very* low barrier reactions in the diffusion limit, there can be significant nonequilibrium in the stable states; this has been treated elsewhere.[4]

For *very* low friction, the stable states should be defined by surfaces of *energy* and not of position as in this section. The appropriate variable is energy (and possibly phase) and not position and momentum.[32] Indeed, this was our approach in Sec. III for the low density case. It may be possible to construct interpolation formulas connecting the two regimes,[31,61] but this requires caution. First, the reaction mechanism may change between the limits.[62] Second, it is not clear that $1D$ reaction models which are valid for high density remain valid at low density. Dimensionality and multiple degrees of freedom can play a dramatic role in, for example, low density isomerizations. They can significantly reduce nonequilibrium effects associated with repeated passage across a barrier top prior to energy stabilization.[63] Such aspects should be examined before reliable interpolation formulas can be constructed.

Finally, when a reactive step is sufficiently fast, as in electron and proton transfer, the rate constant de-

pends upon *static* solvent fluctuations[64] in contrast to the dynamical fluctuations treated here. A different approach for these cases is required.[64]

V. DIFFUSION REGIME REACTIONS IN SOLUTION

In Sec. IV, we focused on the "inertial" regime for reactions in solution. Here we turn to the limit where velocity relaxation is rapid (high friction) and spatial diffusion plays a key or even dominant role. We discuss diffusive structural isomerization and diffusion-influenced pseudobimolecular solution reactions. As the SSP approach to these cases has been extensively described elsewhere,[4,5] we briefly focus only on those aspects deserving of special attention.

A. Diffusion-"controlled" reactions

Many chemical reactions and energy transfer processes in solution depend upon the rate of diffusive approach of the reactants prior to the nondiffusive, short range reactive step. In the SSP, the stable chemical states correspond to[5] (a) an outer spatial region, i.e., reactant separation beyond the range of short range chemical forces responsible for reaction, and (b) an inner region characterized by a potential well of the products. The intermediate zone will often, but need not, be characterized by a potential barrier.[5,62]

The SSP expresses the overall rate constant as[5,65]

$$\kappa_f^{-1} = \kappa_{eq}^{-1} + \kappa_D^{-1} \,. \tag{5.1}$$

Here κ_D is the rate constant for the relative reactant *diffusive* motion up to the stable reactant–intermediate region interface S_R (often a spatial separation $\equiv \sigma$). It accounts for the *spatial* nonequilibrium in the stable reactant and has been extensively discussed elsewhere.[5] The barrier rate constant

$$\kappa_{eq} = \int_0^\infty dt \langle j_i(S_R) j_o^*(S_P, t)\rangle_R \tag{5.2}$$

governs the actual reactive step of formation of products starting from the stable reactant surface $S_R = \sigma$ (where the reactants are caged[5]).

The molecular expression (5.2) replaces empirical parameters used in the past for solution reactions.[5] It can be studied[12] by analytic and numerical simulation techniques focused *solely* on the dynamics of reactants at small separation where reaction occurs; this avoids the necessity of simultaneously monitoring the slow and excursive reactant motion at larger separations.[62] This important feature renders molecular dynamics computer simulation of κ_{eq} tractable.

B. Structural isomerization

The high friction diffusive limit for barrier crossing reactions in solution is not easily attained (cf. Sec. IV). Isomerizations involving motion of large, massive groups over a broad barrier in viscous molecular solvents appear to be the best candidates for this special limit.[4,66]

Northrup and Hynes showed that the SSP result for the diffusive isomerization rate constant is the spatial flux tcf expression[4]

TABLE III. Ratio of the true rate constant to that assuming constant D.

$D(x)$[a]	$\kappa_f/\kappa_f(D_R)$	$\kappa_f/\kappa_f\,[D(0)]$
$D_+(x)$	1.25	0.625
$D_-(x)$	0.42	0.625
$D_+(2x)$	1.09	0.543
$D_-(2x)$	0.36	0.543

[a]Compare Eq. (5.5). The asymptotic values of D_+ are D_0 as $x \to -\infty$ and $3D_0$ as $x \to \infty$; these are reversed for D_-. These values are reached to within 50% at $x = \pm(2/\beta\mu\omega_b^2)^{1/2}$ for $D_\pm(x)$ and to within 25% at the same locations for $D_\pm(2x)$.

$$\kappa_f = \int_0^\infty dt \langle j_i(S_R) j_0^*(S_P, t)\rangle_R = \left[Q_R \int_{S_R}^{S_P} dx\, e^{\beta U(x)} D^{-1}(x)\right]^{-1} . \tag{5.3}$$

Here $D(x)$ is the diffusion coefficient along the reaction coordinate x and $U(x)$ is the potential energy. To simplify Eq. (5.3), we assume that $U(x)$ is symmetric about the barrier top $x = 0$ and that the reactant well and barrier potentials are harmonic to give, for $\beta E_0 \gtrsim 5$,

$$\kappa_f = (\beta\mu\omega_R^2/2\pi)^{1/2} e^{-\beta E_0} \times \left[\int_{-\infty}^{\infty} dx\, D^{-1}(x) \exp\{-\beta(\mu/2)\omega_b^2 x^2\}\right]^{-1} . \tag{5.4}$$

The point we wish to stress has already arisen in Secs. III and IV: The rate constant depends on activation and deactivation on *both* sides of the barrier top. Assuming that κ_f is determined only by events on the nominal reactant side ($x < 0$) of the barrier clearly leads to an error by a factor of 2 if $D = \text{constant}$.[67] The SSP result correctly accounts for the feature that the entire intermediate region determines κ_f.

The intermediate region symmetry can be broken in an interesting way when $D = D(x)$; such x dependence can arise when the molecule changes shape in the reaction.[68] We can examine this via Eq. (5.4) for simple models which correspond, respectively, to increasing and decreasing D as x increases:

$$D(x) = D_+(x) \equiv D_0\{2 + \tanh[(\beta\mu\omega_b^2/2)]^{1/2} x\} \,, \tag{5.5a}$$

$$D(x) = D_-(x) \equiv D_0\{2 - \tanh[(\beta\mu\omega_b^2/2)]^{1/2} x\} \,. \tag{5.5b}$$

Table III shows the results compared to those based on a constant D value taken either as (a) that of the stable reactant ($\equiv D_R$) or (b) the value at the barrier top $x = 0$ [$\equiv D(0)$]. (Both are common approximations.) The importance of the intermediate region, as opposed to just the barrier top $x = 0$, is again clearly revealed. The Table III entry $\kappa_f[D_-(x)]/\kappa_f(D_R)$ is particularly instructive: κ_f is dramatically overestimated by $\kappa_f(D_R)$. According to the SSP result [Eq. (5.4)], the *forward* rate constant κ_f is significantly reduced and mainly determined by the slow diffusion on the side of the barrier towards *products*.

VI. SUMMARY

The power and scope of the SSP approach to reaction rate constants has been demonstrated by application to a

broad range of chemical reaction models. Here we summarize our results.

For gas phase bimolecular reactions, the SSP tcf rate constant formulas were shown to be dynamical implementations of reaction trajectory calculations; the advantages of the SSP results were discussed (Sec. II A). Computationally efficient tcf formulas based on saddle point initial conditions were also presented (Sec. II B) and the connection to transition state theory was made (Sec. II C).

For gas phase unimolecular reactions, we showed that the SSP approach can be readily exploited to find rate constants in the limits of large (Sec. III A) and small (Sec. III B) energy transfer per collision. In both cases, the SSP includes the important role of dynamics occurring away from the reaction threshold. In the energy diffusion limit (Sec. III B), this leads to a correction by a factor of 2 of a standard result. In both this limit and in the large energy transfer regime, the SSP results display clearly the often overlooked feature that a rate constant is typically determined by dynamics on *both* the reactant and product sides of a barrier or energy threshold (Sec. III C).

For barrier crossing reactions in solution, the SSP approach was applied to a non-Markovian generalized Langevin description of the dynamics (Sec. IV A). The major result was obtained that the rate constant depends on the frequency component of the dynamical friction at the reactive frequency [Eqs. (4.24) and (4.28)]. This result frees solution phase reaction rate theory from the unrealistic confines of a macroscopic Brownian motion description. Various realistic friction models were shown to lead to dramatic departure from the standard constant friction predictions of Kramers (Sec. IV D).

When spatial diffusion plays a key role in solution reactions, the SSP approach provides both a natural separation of the slow diffusive step from the short range, nondiffusive intrinsic reaction step and a molecular rate constant expression for the latter (Sec. V A). For diffusive barrier crossings, the SSP formulas naturally reflect the importance of dynamics on both the reactant and product sides of the barrier top. This was illustrated for a model case where the forward rate constant is dominated by slow diffusion on the nominal product side of the barrier (Sec. V B).

APPENDIX A

Here we obtain Eq. (3.7). The P production rate constant in $d\rho_P/dt = \kappa_f \rho_P$ is Eq. (3.6). We must therefore evaluate

$$\kappa_f = \sum_{l\in I}\sum_{m\in I} \omega_{R,m}^{eq} \int_0^\infty dt\, \rho_l^*(t|m)\omega_{lP} , \tag{A1}$$

where $\rho_l^*(t|m)$ is the probability at time t of being in level l of I, given that state m of I was initially occupied. No transitions into I are allowed in the dynamics of $\rho_l^*(t|m)$. Here $\omega_{Rm}^{eq} = \sum_{l\ R} \rho_l^{eq}\omega_{lm}$, where $\rho_l^{eq} = e^{-\beta\epsilon_l}/Q_R$.

To determine $\int_0^\infty dt\, \rho_l^*(t|m)$, we integrate the appropriate kinetic equations

$$\partial\rho_l^*/\partial t = -Z\rho_l^* + \sum_{j\in I} Z\rho_l^{eq}\rho_j^* - \omega_l\rho_l^* ,$$

$$\rho_l^*(t=0) = \delta_{lm} \tag{A2}$$

to find

$$\int_0^\infty dt\, \rho_l^*(t|m) = (Z+\omega_{lP})^{-1} \times \left[\delta_{lm} + Z\rho_l^{eq}\int_0^\infty dt\, \rho_I^*(t|m)\right] , \tag{A3}$$

where $\rho_I^*(t|m)$ is the sum of $\rho_l^*(t|m)$ over all states l in I. Summation of Eq. (A3) over l states in I gives

$$\int_0^\infty dt\, \rho_I^*(t|m) = [(Z+\omega_{mP})(1-\gamma)]^{-1} , \tag{A4}$$

where we have defined

$$\gamma = \sum_{j\in I} Z\rho_j^{eq}(Z+\omega_{jP})^{-1} . \tag{A5}$$

Insertion of Eq. (A4) into Eq. (A3) gives $\int_0^\infty dt\, \rho_l^*(t|m)$, which when inserted into Eq. (A1) yields, after some algebra,

$$\kappa_f = (1-\gamma)^{-1}\kappa_f' , \tag{A6}$$

where κ_f' is the RRKM result [Eq. (3.6)]. If K_I is the equilibrium constant for the formal reaction $R \rightleftharpoons I$, Eq. (A5) shows that, for $\beta E_0 \gg 1$,

$$\gamma \leqslant \sum_{j\in I}\rho_j^{eq} = (1+K_I)^{-1}K_I \ll 1 \tag{A7}$$

and Eq. (A6) reduces to Eq. (3.6).

As noted in I, the *population* tcf can also be used to determine the rate constant. For the present model, it is found that Eq. (3.6) holds when $\beta E_0 \gg 1$.[64(b)]

APPENDIX B

Here we sketch the derivation of the rate constant results quoted in Sec. III B. Equation (3.22) for κ_f may be obtained by direct evaluation of Eq. (3.21) by the methods of Ref. 4. A simpler approach[4] is to integrate the action flux $j = -D[(\partial/\partial J) + \beta\omega]\rho$ from the lower (J_l) to the upper (J_d) stable state surfaces and impose the absorbing BC $\rho(J_d) = 0$. Since j is constant with respect to J in the steady state, we find

$$j(t) = \left[\int_{J_l}^{J_d} dJ\, R(J)\right]^{-1} e^{\beta E_d}\rho(J,t) , \tag{B1}$$

where $R^{-1}(J) = D(J)\, e^{-\beta E(J)}$. The stable state assumption is $\rho(J_s,t) = \rho_R^{eq}(J_s)\rho_R(t)$. With Eq. (B1), this gives the rate law $j(t) = \kappa_f\rho_R(t)$, with κ_f given by Eq. (3.22).

We next consider the derivation of Eq. (3.27). By Eq. (3.25), κ_R^{-1} equals $[\rho_R^{eq}(J_s)]^{-1}\delta\hat{\rho}^0(J_s,J_s;\epsilon=0)$. The Laplace transform of the deviation $\delta\rho^0$ of the distribution ρ from its equilibrium value ρ^{eq} is to be calculated from Eq. (3.14) with a delta function source at $J=J_s$ and reflecting wall BC's applied at $J=J_s$ and $J=0$. To simplify the problem, we *replace* the lower reflecting BC by the assumption of equilibrium: $\rho(J=0) = \rho_R^{eq}(J)$. This will be an excellent approximation except when $\beta E_d \lesssim 2$. (If required, the exact solution can be found.) The problem of finding κ_R is now identical to that solved in Ref.

4 for spatial diffusion; Eq. (3.27) results.

Note that Eq. (3.30) is also the rate constant determined from the population tcf.[3,4,64(b)]

APPENDIX C

The first step in the evaluation of Eq. (4.10) is the elimination of the time integral. Since $v\rho(a, v, t|-a, v_0, 0)$ is the flux into the stable product state, the integrated flux

$$\int_0^\infty dt \int dv\, v\, \rho(a, v, t|-a, v_0, 0) = \lim_{t\to\infty} P(x>a, t|-a, v_0) \equiv \lim_{t\to\infty} P_{RX}(t|-a, v_0) \tag{C1}$$

is the total probability of reaction, given the initial conditions $(x_0 = -a, v_0)$. The reaction probability $P_{RX}(t|-a, v_0)$ can be obtained directly by integration of the full distribution (4.14) to give

$$P_{RX}(t|-a, v_0) = \int_a^\infty dx \int_{-\infty}^\infty dv\, \rho(a, v, t|-a, v_0) = \int_a^\infty dx\, (\pi Q_{11})^{-1/2} \exp(-y_1^2/Q_{11}) , \tag{C2}$$

which works out to be

$$P_{RX}(t|-a, v_0) = \tfrac{1}{2}\,\mathrm{erfc}\left[\frac{a(1+C_{11}) - v_0 C_{12}}{\sqrt{Q_{11}}}\right] . \tag{C3}$$

Here erfc is the complementary error function, Q_{11} is twice the mean square fluctuation in the displacement (4.16), and C_{11} and C_{12} are defined in Eq. (4.17). With Eq. (C3), the integration over v_0 in Eq. (4.14) can be performed; we find that

$$\kappa = (\sqrt{\pi}\,\beta\mu\, Q_R)^{-1}\, e^{-\beta E_0} \times \lim_{t\to\infty} \left\{ C_{12}\phi \exp\left[\frac{\beta\mu a^2\omega_b^2}{2} - a^2\phi^2(1+C_{11})^2\right]\right\} , \tag{C4}$$

where $\phi^{-1} = \sqrt{Q_{11} + (2/\beta\mu)C_{12}^2}$.

Equation (C4) can be considerably simplified by noting that $\sqrt{Q_{11}}$, C_{12}, and C_{11} all diverge in the same way as $t\to\infty$ (cf. Sec. IV B 2). Since κ is independent of a (cf. Sec. IV B 1), we conclude from Eq. (C4) that

$$\lim\phi = \lim\left(\frac{\beta\mu\omega_b^2}{2}\right)^{1/2} C_{11}^{-1} , \tag{C5}$$

and Eq. (C4) simplifies to

$$\kappa = Q_R^{-1}\, e^{-\beta E_0} (\omega_b^2/2\pi\beta\mu)^{1/2} \lim(C_{12}/C_{11}) . \tag{C6}$$

To complete the derivation, we first note from Eq. (4.18) and L'Hospital's rule that

$$\lim(C_{12}/C_{11}) = \lim(C_{22}/C_{21}) = \omega_b^{-2} \lim[d\ln C(t)/dt] . \tag{C7}$$

As discussed in Sec. IV B 3, $C(t) \to C_r e^{\lambda_r t}$ as $t\to\infty$, where λ_r is the reactive eigenvalue. Therefore, Eqs. (C6) and (C7) give

$$\kappa = Q_R^{-1}\, e^{-\beta E_0} (2\pi\beta\mu)^{-1/2} \lambda_r/\omega_b , \tag{C8}$$

which is just Eq. (4.24) with Eq. (4.25). It is noteworthy that a similar derivation shows that the average kinetic energy for reacting particles is just the thermal value.

[1] S. H. Northrup and J. T. Hynes, J. Chem. Phys. **73**, 2700 (1980), preceding paper.

[2] S. H. Northrup and J. T. Hynes, J. Chem. Phys. **68**, 3203 (1978).

[3] S. H. Northrup and J. T. Hynes, Chem. Phys. Lett. **54**, 248 (1978).

[4] S. H. Northrup and J. T. Hynes, J. Chem. Phys. **69**, 5246, 5261 (1978). Professor K. Schulten has pointed out to us an error in the first paper in the evaluation of the internal rate constants κ_R and κ_P. This will be corrected elsewhere; it does not influence the results of the present paper.

[5] S. H. Northrup and J. T. Hynes, J. Chem. Phys. **71**, 871, 884 (1979); Chem. Phys. Lett. **54**, 244 (1978).

[6] Equations (1.4) and (1.5) have certain conditions for their validity which are discussed at length in I. We will restrict their application in this paper to such conditions in Secs. (III.B), (III.C), and (V.B).

[7] See, for example, P. J. Kuntz, in *Dynamics of Molecular Collisions, Part B*, edited by W. H. Miller (Plenum, New York, 1976).

[8] This is closely related to Eq. (A5) of T. Yamamoto, J. Chem. Phys. **33**, 281 (1960). The upper limit Δt in that equation should be interpreted as any time after the collision duration.

[9] J. T. Hynes (unpublished).

[10] W. H. Miller, J. Chem. Phys. **61**, 1823 (1974); **62**, 1899 (1975); P. Pechukas, in Ref. 7; P. Pechukas and F. J. McLafferty, J. Chem. Phys. **58**, 1622 (1973).

[11] R. A. Marcus, J. Chem. Phys. **45**, 4493, 4500 (1966); **49**, 2610 (1968); S. F. Fischer, G. L. Hofacker, and R. Seiler, *ibid.* **51**, 3951 (1969); N. H. Hijazi and K. J. Laidler, *ibid.* **58**, 349 (1973).

[12] R. Grote and J. T. Hynes (work in progress).

[13] J. C. Keck, Adv. Chem. Phys. **13**, 85 (1967); Adv. At. Mol. Phys. **8**, 39 (1972). For recent developments see B. C. Garrett and D. G. Truhlar, J. Phys. Chem. **83**, 1052 (1979) and references therein.

[14] J. B. Anderson, J. Chem. Phys. **58**, 4684 (1973); **62**, 2446 (1975). A related development is the determination of reaction coordinates starting from S_s; see, for example, C. Leforestier, J. Chem. Phys. **68**, 4406 (1978).

[15] C. H. Bennett, in *Algorithms for Chemical Computation*, edited by R. E. Christofferson (American Chemical Society, Washington, D.C., 1977); J. A. Montgomery, D. Chandler, and B. J. Berne, J. Chem. Phys. **70**, 4056 (1979).

[16] Our Eq. (2.13) has already been applied to diffusion limit reactions in S. H. Northrup and J. A. McCammon, J. Chem. Phys. **72**, 4569 (1980).

[17] S. Glasstone, K. J. Laidler, and H. Eyring, *The Theory of Rate Processes* (McGraw-Hill, New York, 1941); E. Wigner, Trans. Faraday Soc. **34**, 29 (1938); J. Horiuti, Bull. Chem. Soc. Jpn. **13**, 210 (1938).

[18] This form can often be convenient for calculation as the fluxes are both across the saddle point surface S_S. Unfortunately, state-to-state rate constants cannot be simply related to the total flux at S_S.

[19] Consider a one dimensional model where $x = 0$ is the saddle point of energy $U(0)$. The integral of the tcf for any $t > 0$ is $\langle j(0)\,\theta(vt)\rangle_R$, where θ is the step function. This is just $Q_R^{-1} e^{-\beta U(0)} \langle v\rangle_+$, which is the TST answer. (The + notation means a positive velocity average.)

[20] Quoted in R. Rosenstein, Ber. Bunsenges. Phys. Chem. **77**, 493 (1973).

[21] R. Kapral, J. Chem. Phys. **56**, 1842 (1972); F. Garisto and R. Kapral, *ibid.* **58**, 3129 (1973); S. Hudson and J. Ross, J. Stat. Phys. **14**, 469 (1976); D. Chandler, J. Chem. Phys. **68**, 2959 (1978).

[22] In the gas phase bimolecular reaction case, nonequilibrium

effects arise from finite translational and vibrational equilibration rates of the stable reactants. Trajectories into I are in fact sampled from nonequilibrium reactant distributions. These effects are typically negligible in the bimolecular case; see, for example, B. Shizgal and M. Karplus, J. Chem. Phys. **52**, 4262 (1970); **54**, 4345 (1971); B. Shizgal, *ibid.* **57**, 3915 (1972). Nonequilibrium effects can often be regarded as equivalent to surface recrossing effects. See Ref. 13 for discussion.

[23]H. S. Johnston, *Gas Phase Reaction Rate Theory* (Ronald, New York, 1966).

[24](a) E. E. Nikitin, *Theory of Elementary Atomic and Molecular Processes in Gases* (Clarendon, Oxford, 1974); (b) W. Forst, *Theory of Unimolecular Reactions* (Academic, New York, 1973).

[25]For recent discussions of models of reactive transition probabilities, see for example, N. C. Blais and D. G. Truhlar, J. Chem. Phys. **65**, 5335 (1977); **70**, 2962 (1979); W. Forst and A. P. Penner, *ibid.* **72**, 1435 (1980).

[26]B. Widom, J. Chem. Phys. **55**, 44 (1971); **61**, 672 (1972); H. O. Pritchard, in *Specialist Periodical Reports, Reaction Kinetics* (Chemical Society, London, 1975), Vol. 1; R. K. Boyd, Chem. Rev. **77**, 93 (1977).

[27]Critical discussion of the strong collision limit has been given in J. Troe, J. Chem. Phys. **66**, 4745, 4759 (1977); and J. Troe and H. Gg. Wagner, in *Physical Chemistry of Fast Reactions* (Plenum, New York, 1973).

[28]The steady state assumption for i in I gives, with Eq. (3.4), $\rho_i(t)/\sum_j \rho_j(t) = Z(\omega_{iP}+Z)^{-1}$ and $\rho_i = \rho_i^{eq}$ in R.

[29]The "M" in RRKM refers[23,24] to a specific model of the ω_{iP}, which we have not specified here. Work in this direction is under way for the cluster sticking probabilities determined numerically in J. W. Brady, J. D. Doll, and D. L. Thompson, J. Chem. Phys. **71**, 2467 (1979).

[30]T. A. Bak and J. L. Lebowitz, Phys. Rev. **131**, 1138 (1963); S. E. Nielsen and T. A. Bak, J. Chem. Phys. **41**, 665 (1964). See also E. E. Nikitin, Discuss. Faraday Soc. **33**, 288 (1962).

[31]J. L. Skinner and P. G. Wolynes, J. Chem. Phys. **72**, 4913 (1980); **69**, 2143 (1978). Important non-Gaussian effects may also arise when solvent motion involves barrier jumping.

[32]H. A. Kramers, Physica (The Hague) **7**, 284 (1940).

[33]See, for example, Ref. 24(a) and J. Keck and G. Carrier, J. Chem. Phys. **43**, 2284 (1965). The role of rotation is quite important in diatomic dissociation; it can lead to an order of magnitude increase in the rate constant in the diffusion limit [M. N. Safaryan, E. V. Stupochenko, and N. M. Pruchkina, Theor. Exp. Chem. **5**, 115 (1969)]. We neglect rotation here only for simplicity; the SSP approach can also handle its inclusion.

[34](a) S. A. Landon and J. C. Keck, J. Chem. Phys. **48**, 374 (1968); M. R. Flannery, Ann. Phys. (N.Y.) **67**, 376 (1971); (b) P. J. Pagni and J. C. Keck, J. Chem. Phys. **58**, 1162 (1973).

[35]A. N. Kaufmann, Phys. Rev. Lett. **27**, 376 (1971); G. M. Zaslavskii and B. V. Chirikov, Sov. Phys. Usp. **14**, 549 (1972); J. O. Eaves and J. T. Hynes (work in progress).

[36]See, for example, D. W. Oxtoby and S. A. Rice, J. Chem. Phys. **65**, 1676 (1976).

[37]Assumption (1) in Sec. III. B. 1 is more difficult to satisfy for the MO, since $\omega \to 0$ as $E \to E_d$. One should really derive a generalized diffusion equation including phase memory to replace Eq. (3.14). See also J. C. Light, J. Chem. Phys. **36**, 1016 (1962); P. Mazur, Physica (Utrecht) **25**, 149 (1959).

[38]Equations (3.20a) and (3.20b) have also been obtained in Refs. 39 and 40 below when $\beta E_d \gg 1$. Equation (3.20b) does not appear in Ref. 32 but is implicit in the development.

[39]T. A. Bak and K. Andersen, Mater. Fys. Medd. Dansk. Vidensk. Selsk. **33**, 109 (1975).

[40]W. Brenig, H. Müller, and R. Sedlmeier, Phys. Lett. A **54**, 109 (1975).

[41]Equation (3.30) is the inverse mean first passage time for dissociation, given an equilibrium distribution in the oscillator.[1,3] It is also equivalent to a result of Brenig *et al.*[40] found by smallest eigenvalue analysis.

[42]For the HO, Eq. (3.30) gives $k_f^{-1} = [\mathrm{Ei}(\beta E_d) - \ln(\beta E_d) - \gamma]$, where Ei is the exponential integral and γ is Euler's constant. A similar formula has been found by P. B. Visscher, Phys. Rev. B **13**, 3272 (1976).

[43]Another route to this result is mentioned in Appendix B.

[44]See, for example, articles by S. Chandrasekhar and M. Wang and G. E. Uhlenbeck, in *Noise and Stochastic Processes*, edited by N. Wax (Dover, New York, 1954).

[45]Kramers' result [Eq. (4.2)] has been repeatedly found to give the rate constant accurately in reaction computer simulations *based on the LE equation* (4.1). Some recent examples are Ref. 4; R. M. Levy, M. Karplus, and J. A. McCammon, Chem. Phys. Lett. **65**, 4 (1979); M. R. Pear and J. H. Weiner, J. Chem. Phys. **69**, 785 (1978); E. Helfand, J. Chem. Phys. **69**, 1010 (1978); J. S. McCaskill and R. G. Gilbert, Chem. Phys. **44**, 389 (1979). An interesting case where Eq. (4.2) fails with LE simulated dynamics is M. P. Allen, "Brownian Dynamics Simulation of a Chemical Reaction in Solution" (preprint); the reaction studied is multidimensional and energy controlled and Eq. (4.2) does not apply.

[46]R. Grote and J. T. Hynes, (a) "Atom Transfer Reactions in Solution"; (b) "Structural Isomerization Reactions in Solution" (to be submitted.)

[47]GLE-type equations are well known in a variety of nonreactive transport and relaxation problems; see, for example, J. T. Hynes and J. M. Deutch, in *Physical Chemistry, An Advanced Treatise* (Academic, New York, 1975), Vol. IIB; S. A. Adelman and J. D. Doll, Acc. Chem. Res. **10**, 378 (1977). The GLE can only be regarded as a model in the absence of any rigorous derivation; see Ref. 48.

[48]J. M. Deutch and I. Oppenheim, J. Chem. Phys. **54**, 3547 (1971); P. Ullersma and J. A. Tjon, Physica (Utrecht) **71**, 294 (1974).

[49]See, for example, J. T. Hynes, Annu. Rev. Phys. Chem. **28**, 301 (1977) and references therein.

[50]On the true potential, there would be ultimate return from regions R and P into region I. However, this is irrelevant for the evaluation of Eq. (4.4), which already contains the information that κ is determined by dynamics in region I.

[51]These statements have been verified by direct numerical examination in the constant friction case and by analytic methods in general. In the former case, the validity holds down to about $\beta E_0 \approx 3$ when internal nonequilibrium becomes important. Caution is required at high friction; the absorbing BC's in Eq. (4.4) should be interpreted as irreversible passage beyond surfaces of small but finite width of the order of the distance traveled during a velocity correlation time ($\approx \mu/\zeta$).

[52]S. Adelman, J. Chem. Phys. **64**, 124 (1976); R. M. Mazo, in in *Stochastic Processes in Nonequilibrium Systems*, edited by L. Garrido, P. Seglar, and P. J. Shepherd (Springer, New York, 1978). The GLE is *not* equivalent to the so-called "retarded" Fokker–Planck equation; cf. E. L. Chang, R. M. Mazo, and J. T. Hynes, Mol. Phys. **28**, 997 (1974) and the references above.

[53]This should be carefully distinguished from the "smallest eigenvalue" often used in kinetics; the latter is the rate constant itself.

[54](a) J. M. Dickey and A. Paskin, Phys. Rev. **188**, 1407 (1969); S. A. Adelman and B. J. Garrison, J. Chem. Phys. **65**, 3751 (1976); A. Rahman, M. J. Mandell, and J. P. McTague, *ibid.* **64**, 1564 (1976); M. Shugard, J. C. Tully, and A. Nitzan, *ibid.* **66**, 2534 (1977); (b) F. H. Stillinger and A. Rahman, J. Chem. Phys. **60**, 1545 (1974); W. F. Edgell, in *Infrared and Raman Spectroscopy*, edited by E. G. Brame and J. Grasselli (Dekker, New York, 1976), Vol. 1A.

[55]H. C. Brinkman, Physica (Utrecht) **22**, 149 (1956); R. J. Donnelly and P. H. Roberts, Proc. R. Soc. (London) Ser. A **312**, 519 (1969).

[56]R. I. Cukier, R. Kapral, J. R. Mehaffey, and K. J. Shin, J. Chem. Phys. **72**, 1844 (1980); S. A. Adelman, *ibid.* **71**, 4471 (1979).
[57]See, for example, P. G. Wolynes, Annu. Rev. Phys. Chem. **31**, (1980) (in press) and references therein.
[58]J. M. Schurr, Chem. Phys. **45**, 119 (1980); S. Harris, Mol. Phys. **26**, 953 (1973); M. J. Stephen, J. Chem. Phys. **55**, 3878 (1971).
[59]See, for example, E. M. Kosower, *An Introduction to Physical Organic Chemistry* (Wiley, New York, 1968).
[60](a) P. A. Schofield, "Inelastic Scattering of Neutrons," Proceedings of the Symposium in Vienna 1960, Vol. 1, p. 39; (b) J. T. Hynes, R. Kapral, and M. Weinberg, J. Stat. Phys. **13**, 427 (1975); (c) A. Rahman, Phys. Rev. Sect. A **136**, 405 (1964); (d) G. D. Harp and B. J. Berne, J. Chem. Phys. **49**, 1249 (1968) (we thank Professor P. G. Wolynes for recalling this reference to our attention); (a) J. A. McCammon, P. G. Wolynes, and M. Karplus, Biochemistry **18**, 927 (1979); (f) M. Pagitsas, J. T. Hynes, and R. Kapral, J. Chem. Phys. **71**, 4492 (1979).
[61]J. Troe, in *Physical Chemistry, An Advanced Treatise* (Academic, New York, 1975), Vol. VIB; also in *High Pressure Chemistry*, edited by H. Kelm (Reidel, Dordrecht, 1978); P. B. Visscher, Phys. Rev. B **14**, 347 (1976).
[62]J. T. Hynes, R. Kapral, and G. M. Torrie, J. Chem. Phys. **72**, 177 (1980).
[63]X. Chapuisat and Y. Jean, J. Am. Chem. Soc. **97**, 6325 (1975); A. Warshiel and M. Karplus, Chem. Phys. Lett. **32**, 11 (1975).
[64](a) See, for example, J. Ulstrup, *Charge Transfer Processes in Condensed Media* (Springer, Berlin, 1979) and references therein; (b) J. T. Hynes and S. H. Northrup (in preparation).
[65]A simple derivation along the lines of Sec. IV of I also gives Eq. (5.1). Consider the reaction scheme $A+B \rightleftarrows [A+B]_\sigma \rightarrow C$, with rate constants κ_D, κ_{-D}, and κ_i, involving the "caged" reactant pair at separation σ and at "bulk" separations. Steady state analysis on $[A+B]_\sigma$ gives κ_f as $\kappa_f = (\kappa_i + \kappa_{-D})^{-1}\kappa_i\kappa_D$. The ratio κ_D/κ_{-D} is the "equilibrium constant" for separation σ and for any typical bulk separation. This is the equilibrium pair distribution $g(\sigma)$, so that $\kappa_D = g(\sigma)\kappa_{-D}$. Together with the identity $\kappa_{eq} = g(\sigma)\kappa_i$,[5] this gives Eq. (5.1).
[66]This limit has been adopted for several simulations of polymer dynamics; see, for example, M. Fixman, J. Chem. Phys. **69**, 1527 (1978); G. T. Evans and D. C. Knauss, *ibid.* **72**, 1504 (1980); M. J. Pear and J. H. Weiner, *ibid.* **71**, 212 (1979). E. Helfand, Z. R. Wasserman, and T. A. Weber, *ibid.* 70, 2016 (1979).
[67]This feature appears not to be generally appreciated; see, for example, I. Procaccia and J. Ross, J. Chem. Phys. **67**, 5565 (1977).
[68]D. C. Knauss and G. T. Evans, J. Chem. Phys. **72**, 1499 (1980).